NAL TM-333T

UDC 620.178.3:
539.43:
629.73.02.018.4

TECHNICAL MEMORANDUM OF NATIONAL AEROSPACE LABORATORY

TM-333T

Review of Aeronautical Fatigue Investigation in Japan 1975-1977

Tadao KAMIYAMA, Kazuyuki TAKEUCHI,
Soshiro IIDA, Kosaburo YAMANE and Hiroo ASADA

July 1977

NATIONAL AEROSPACE LABORATORY

CHŌFU, TOKYO, JAPAN

TABLE OF CONTENTS

Review of Aeronautical Fatigue Investigation in Japan 1975-1977 *

Tadao KAMIYAMA,** Kazuyuki TAKEUCHI,***
Soshiro IIDA,**** Kosaburo YAMANE**** and Hiroo ASADA****

概　　要

国際航空機疲労会議の第15回会議は，昭和52年5月に西ドイツのダルムシュタットにおいて開催された。

この会議において，日本における最近2年間の航空機疲労に関する研究の展望を発表するために，関係ある方々のご協力をえて作成したのが，本報告である。

1. INTRODUCTION

After the fourteenth meeting of the ICAF, for the purpose of co-ordinating to the ICAF activity in Japan, the 129th Committee on Strength, Fracture and Fatigue (The chairman; T. Yokobori) of the Japan Society for Promotion of Science has reorganized the members of this Sixth Sub-Committee on Aeronautical Fatigue as follows:

The chairman of sub-committee: T. Kamiyama

The secretary of sub-committee: K. Takeuchi

and the other eighteen members consist of professors in universities, researchers in government laboratories, airplane manufactuers, airline operators and others who are working on the aeronautical fatigue problems. The sub-committee has agreed to collect the Japanese author's papers concerning aeronautical fatigue and distribute to the ICAF member countries from National Aerospace Laboratory, The Science and Technology Agency, Japan.

Nineteen papers written in English, most of which were concerning the basic fatigue problems studied in universities, have already been distributed to ICAF member countries. The titles of those ICAF Documents presented by Japanese authors are listed in the reference at the end of this review.

The Model 700, a twin engine general usage airplane has been developed by Fuji Aircraft Division and General Aviation Division of Rockwell International. The full scale fatigue test of this prototype is now underway at the Fuji Heavy Industries, Ltd., in Utsunomiya, Japan. The full scale fatigue test of Shinmeiwa PS-1 flying boat was conducted in 1975 and the fatigue test of landing gear of Shinmeiwa US-1 that is the amphibious version of the PS-1 was conducted in 1976 at The Third Research Center, T.R.D.I., Japan Defence Agency.

In Japanese civil aviation, there were forty three accidents in 1975 and fifty six accidents in 1976. The analyses of those accidents identified that the main causes of four accidents in 1975 and two accidents in 1976 were due to the fatigue.

This paper is the review of the investigation on aeronautical fatigue problems in National Aerospace Laboratory, The Third Research Center and three representative airplane manufactures, Fuji, Mitsubishi and Kawasaki.

---

* Received June 24, 1977.

** The Aircraft Accident Investigation Commission

*** First Airframe Division

**** Second Airframe Division

Presented at the 15th Meeting of the International Committee on Aeronautical Fatigue, held on May 9 – May 13, 1977 at Darmstadt, Germany.

2. NATIONAL AEROSPACE LABORATORY, THE SCIENCE AND TECHNOLOGY AGENCY, JAPAN

2.1 On the Data Collection of Gust Loads

1) Background

Gust load collections in Japan were conducted twice in the past, in response to the request of ICAO Airworthiness Committee. In both studies, scratch-type flight recorders for accident investigation were used to obtain the flight data. The former study was conducted around 1960, collecting the gust loads encountered by DC-4 transports in domestic scheduled flights and the frequencies of derived gust velocities were obtained. The latter study was continued from Sept. 1973 to Aug. 1975 and six extreme events were collected encountering severe turbulences by transports in scheduled flights. The result of the analysis was reported to ICAO Airworthiness Com mittee in 1976 (NAL TM-319T, 11/1976). The typical records of discrete and continuous turbulence among them are shown in Fig. 1 and Fig. 2, respectively.

On the other hand, current large jet-transports have been equipped with the DFDR (Digital Flight Data Recorder). Although the installation of the DFDR is originally obligated by airworthiness regulations for accident investigation, the records of the DFDR's in daily operations contain the useful information on flight loads, and can also be available to obtain those statistical data with the aid of high speed digital computers.

National Aerospace Laboratory, therefore, has started to collect the gust data in domestic scheduled flights by the DFDR's which are equipped on Lockheed L-1011 transports of All Nippon Airways. In the following sections, the method of processing data and some results are presented.

2) Computer Processing of DFDR Data

First, the records of the DFDR are reproduced and searched to find the regions of gust encounters (the patches of turbulence). When a patch of turbulence is identified, the informations on the turbulence patch like mean altitude and airspeed, level crossing frequencies of vertical accelerations, patch length, etc. are output on card together with the flight identification data and the information of flight time at each altitude band.

Finally, when sufficient data are stored, the statistical gust data are summarized in the form of frequencies per hour of vertical accelerations and derived gust velocities, values of P_1, P_2, b_1 and b_2 in the gust PSD method, variations of those values with altitudes, seasons and routes, correlations between vertical and lateral accelerations and between gust encounters and the variation of air temperature, etc.

The patch of turbulence is identified out of the whole records by the computer, monitoring the time history of vertical accelerations with the following steps:

i) The upper and lower threshold levels (UTL and LTL) and preset above and below the mean level (1 g level flight), respectively.

ii) The records are searched to find the region where the vertical accelerations cross the UTL and LTL continuously. If the vertical accelerations stop crossing the thresholds more than 30 seconds, then it is regarded as the end of the turbulence patch.

iii) If the vertical accelerations stay above the UTL or below the LTL more than 10 seconds, that portion is not regarded as the patch of turbulence in order to exclude the pilot maneuvering.

iv) The beginning and ending of the turbulence patch thus found is finally modified by the points where the vertical accelerations cross 1 g mean level just before and after the first and the last crossing of the threshold, respectively.

In this study, the values of the threshold levels are programmed to be variable from 1 g ± 0.08 g to 1 g ± 0.2 g. The levels at every 0.05 g are used to count the level crossing frequencies of vertical accelerations in the turbulence patch.

3) Results of Analysis

In order to check the validity of the computer software for data processing and to investigate the effect of the threshold levels on the turbulence identification, the DFDR records of 300 flight hours were processed by the method explained in the previous section. The data contained 201 flights which were equivalent to the flight distance of 225,600 kilometers. The maximum and minimum vertical accelerations in the whole records were 1.61 g and 0.21 g, respectively.

The cumulative frequencies of derived gust velocities at an altitude band from 3,000 to 6,000 meters

are shown in Fig. 3. The vertical lines represent the ranges of variation of the frequencies of derived gust velocities when the values of the threshold levels are changed from 1g ± 0.08g to 1g ± 0.2g. As a reference, the value adopted in MIL specifications in U.S.A. is shown by the solid curve. It is noted from Fig. 3 that the frequencies over 5m/sec (15ft/sec) does not depend on the value of the threshold levels. The same results of the effect of the thresholds on the derived gust frequencies have been obtained for other altitude bands of 300 ~ 3,000, 6,000 ~ 10,000 and 10,000 ~ 13,000 meters.

Fig. 4 shows the percentage of the flight time in the patch of turbulence explained in the previous section to the total flight time. The horizontal lines indicate the ranges of variation of the percentage when the values of thresholds are changed from 1g ± 0.08g to 1g ± 0.2g. As a reference, the value of P_1 (percentage of flight time in non-storm turbulence) adopted in U.S.A. MIL specification is shown by the solid curve. As shown in the figure, the percentage of the flight time in the turbulence patch is highly dependent on the values of threshold.

4) Concluding Remarks

The DFDR records of 300 flight hours were analysed to obtain the gust statistical data from the experience of transports in daily operations. The results have clarified the availability of the DFDR for gust data collection by computer processing. It has also been noted that the frequencies of derived gust velocities over 5m/sec does not depend on the value of the threshold levels used for the turbulence patch identification, whereas the percentage of the flight time in the turbulence patch to the total flight time is highly dependent on it.

It is expected from the present study that the DFDR will also be available to obtain other airplane airworthiness data, i.e., maneuvering and landing loads, wind shear, statistical distributions of airplane speeds in operation against the target speeds, etc.

2.2 Preliminary Studies on Fatigue Load and Test Method

For the purpose of estimating fatigue life of airplane structure under more realistic fatigue test load, NAL makes an effort to develop the system which can generate flight-by-flight load and perform fatigue test with a minicomputer control. As the test has just started, in this section, the procedure of determination of light load, the simulation technique and the test apparatus are described.

Recently, The Standardized Load Program was proposed by LBF and NLR (LBF-BERICHT FB-106 and NLR TR 73029U, 3/1973). This program is based on many calculated and measured data, and the results which were investigated over the last decades are contained in this program. The peak distribution of this program is refered when the following program is studied.

Considering the lower skin of wing root which is thought to be the critical component of airplane structures, the representative fatigue loads are gust loads and ground-air-ground loads. The gust process is generally modeled as a composite Gaussian process (MIL-A-008861A (USAF), 3/1971). In detail, the continuous turbulence consists of a series of gust patches and each patch is a stationary Gaussian random process. If the standard deviation stands for the intensity of patch, the distribution is shown by adding half Gaussian probability density functions with the parameters C_1, C_2, σ_{x1} and σ_{x2}. C_1 and C_2 represent the fractions of non-storm and storm respectively with the intensities σ_{x1} and σ_{x2}. When only the term T that an airplane encounters air turbulence is taken into consideration, the sum of C_1 and C_2 becomes unity. If the response of airplane structure is assumed to be linear, σ_{x1} and σ_{x2} can be replaced by σ_{y1} and σ_{y2} which are the intensities of response of critical component due to non-storm and storm. On the other hand, the Gaussian random process $y(t)$ with mean zero and its power spectral density $S_y(\omega)$ can be simulated by way of the sum of cosine functions.

In order to simulate the process, the parameters C_1, C_2, σ_{y1} and σ_{y2} must be determined. Essentially, these values can be established by the mission analysis of the airplane. However, in the present test, investigating many references and also considering The Standardized Load Program, the values listed below are adopted.

$C_1 = 0.995$, $C_2 = 0.005$, $\sigma_{y1} = 0.126$g, $\sigma_{y2} = 0.324$g

The intensity distribution is divided into 30 segments of ${}_1\sigma_y = 0.009$g, ${}_2\sigma_y = 0.027$g, ..., ${}_{30}\sigma_y = 0.531$g with $\Delta\sigma_y = 0.018$g. The lower four segments from ${}_1\sigma_y$ to ${}_4\sigma_y$ are omitted because of the less contribution to fatigue life and the shortening of test period.

The stress of 1g level flight is 7 kg/mm^2 and the ground load is -0.5 times of 1g flight load. It is assumed that T is 300 sec which corresponds to 8.3% of one hour flight, i.e., short range operation. For the sake of generation of random process, the bending moment spectral density of C-5A at the wing root presented by R.L. McDougal (Meeting of Aircraft Response to Turbulence, NASA Langley Research Center, 9/1968) is utilized (Fig. 5). Investigating this spectrum, the frequency resolution (Δf) and the number of division (n) are taken as 0.01 Hz and 256 respectively. Therefore, the simulation period is 100 sec.

The test apparatus mainly consists of MTS closed loop servo-hydraulic fatigue machine and HP-2100 Digital Minicomputer which is microprogramable. The arrangement of these apparatus, 12 bits Digital-Analogue Converter and the softwares which are used for the test are developed by NAL. It should be notes that the grips and anti-buckling guides recommended by Schijve (NLR TR 68117U, 12/1968) are adopted. The computer unit with 16K memory of 16 bits word has Time Base Generator, PTR, TTY, ADC, DAC (2 channels of 8 bits), Relay Register, Writable Control Store (RAM) and Programable ROM Writer. The calculation is carried out by integer, and all data which are previously stored in the memory are called by the addressing technique. Applying the microprogram in order to generate pseudo ramdom numbers and random processes, the test time becomes a quarter of the real time. Fig. 6 shows the example of flight-by-flight loads. The distribution of maxima and mean cross peak which are corresponding to 2,000 flights are given in Fig. 7.

According to the results, the numbers of peaks in the middle level are larger than those of The Standardized Load Program. It is possible to bring the former distribution close to the latter by altering the parameters C_1, C_2, σ_{y1} and σ_{y2}, and the higher and lower truncation level of intensity distribution. Although, at present, the fatigue test is performed in order to investigate the fatigue process on crack initiation and propagation, it is necessary to find the reasonable parameters and truncation level mentioned above and compare the test results with those obtained by The Standardized Load Program.

2.3 Relation between Scatter of Fatigue Life and S-N Curve

The equivalent stress is defined as the sum of the applied stress and the error in applied stress. This concept is applied to the results of series of fatigue tests on 2024-T4 aluminium alloy specimens with a circular hole ($K_t = 2.54$) and a sharp notch ($K_t = 8.25$) at constant temperature and humidity. Fig. 8 and Fig. 9 show the fatigue life distribution for $K_t = 2.54$ and 8.25 respectively. The interrelation between the scatter of the equivalent stress, the S-N curve, where N is the median fatigue life, and the scattering of fatigue life is discussed.

The main results of this study are:

(1) The fatigue crack initiation period of the specimen with a circular hole is about 2% of fatigue life at the applied stress 26kg/mm^2. When an applied stress is lowered, it becomes longer. It is about 76% of fatigue life at the applied stress 12.5kg/mm^2.

On the other hand, the microscopical observations indicate the fatigue crack grown throughout most of the whole life of a specimen with a sharp notch, when an applied stress is higher than or equal to 8kg/mm^2. When an applied stress is not higher than 7kg/mm^2, the fatigue life is covered by the two periods of fatigue nucleation and propagation.

(2) In the stress range where the shape and slope of the S-N curve are almost identical, shown in Fig. 10, the distribution shape and scatter of fatigue life obtained from experiment are similar regardless of stress level and notch configuration. The gentler the slope of the S-N curve, the larger the scatter of fatigue life becomes.

(3) The equivalent stress is distributed almost in a normal distribution, and its standard deviation is nearly constant ranging from 0.25 to 0.38kg/mm^2 regardless of stress level and the ratio of crack nitiation period to fatigue life.

(4) In the stress range where the S-N curve on a semi-logarithmic scale is nearly straight, the fatigue life is distributed in a log-normal distribution, which agrees with the results for unnotched specimen reported in ICAF Doc. No. 800.

2.4 Parameter Estimation of Weibull Distribution using Test Results obtained in Japan

As is well known, the log-normal and Weibull distribution can empirically define the distribution of fatigue life and both are utilized to the design and reliability analysis of airplane structures.

In Japan, the scatter factors of transport airplane structures have been determined by the log-normal distribution. The standard deviation of aluminium alloy structure was recently estimated to be 0.154 from 62 groups of fatigue tests with 95% confidence level.

It should be noted that the significant difference between those distributions in the lower tails has an important influence to the result of reliability analysis.

Although the Weibull distribution, in general, has three parameters which are shape (α), scale (β) and location parameter (δ), the location parameter (minimum life) is usually taken as zero. On the other hand, it is pointed out that the long life transport has a minimum life, and introducing this minimum life value, the scatter factor becomes smaller. In case of the parameter estimation of two-parameter Weibull distribution, it is shown that the first two ordered statistic estimation method (FTOSE) proposed by N.R. Mann (Technometrics, Vol. 10, 5/1968) and applied by I.C. Whittaker, et al. (AFML-TR-69-65, 3/1969) is more effective than the maximum likelihood estimation. However, it is thought that there is no suitable method to estimate three parameters of Weibull distribution. Therefore, it is tried to apply the extended FTOSE and Bayesian method for the parameter estimation.

In order to derive the probability density function of Z = (second failure) / (first failure), a new assumption must be introduced. In this case, it is assumed that the parameter $\epsilon = \delta/\beta$ as well as shape parameter α are constant.

For the estimation of α and ϵ of aluminium alloy structural components, the case of sample size n = 3 is taken, because this group is the largest which is equal to 41. The fatigue test results are listed in Table 1 with the fatigue lives of first and second failure and Z. The distribution of Z is plotted in Fig. 11. Although the relation between α and ϵ is represented in Fig. 12, unfortunately the most probable value cannot be determined by this method.

Table 2 shows the safe and reasonable values of α and ϵ of each material which are recommended by A.M. Freudenthal (AFML-TR-74-198, 4/1975). In this table, the short life and the long life are corresponding to fighter and transport respectively.

As the method mentioned above introduces the uncertain values of α and ϵ, it is tried to make use of the Bayesian method for the sake of finding more reliable values. If the values for long life listed in Table 2 are reasonable, it is expected that they will become the mode of posterior probability density function.

Considering a prior probability for this analysis, there is no information about α and ϵ which are mutually independent. Therefore, it is assumed that its density function is constant over the range of $\alpha_{min} \leqslant \alpha \leqslant \alpha_{max}$ and $0 \leqslant \epsilon \leqslant \epsilon_{max}$. These ranges must be sufficiently chosen by investigating the results of posterior probability density. On the other hand, the likelihood function is derived with the assumption that the samples $Z_1, Z_2, \ldots, Z_m$ are mutually independent.

In case that the same data which are utilized in the former analysis are taken and each value in the calculation is gven as follows;

$\alpha_{min} = 0.5$, $\alpha_{max} = 5.0$, $\Delta\alpha = 0.1$, $\epsilon_{max} = 0.4$, $\Delta\epsilon = 0.01$

the posterior probability distribution is shown in Fig. 13, and its mode is $\alpha = 3.6$ and $\epsilon = 0.02$ which means that the minimum life is 2% of the scale parameter. These are almost the same as the values recommended by Freudenthal. The relation of α and ϵ in Fig. 12 is approximately corresponding to the ridge of this distribution. Although the group size is very small and only the sample size n = 3 is examined, the Bayesian method is applicable to estimate the parameters of Weibull distribution.

2.5 Plane Bending Fatigue Strength of CFRP Aluminum Honeycomb Sandwich

The experimental investigation on the plane bending fatigue strength of a honeycomb sandwich beam consisting of an aluminum honeycomb core and carbon fiber reinforced plastics facing was conducted. Fig. 14 shows the S-N curve for CFRP aluminum honeycomb sandwich.

It was found that the aluminum honeycomb sandwich beam with CFRP facing has a considerably higher strength in plane bending fatigue than FRP honeycomb sandwich specimen with GFRP (glass fiber re-

inforced plastics) facing, and that the plane bending fatigue strength of the honeycomb sandwich beam depends deeply on the properties of the facing materials.

2. 6 Studies on Acoustic Fatigue

Experimental study of acoustic fatigue on bond-riveted panel specimen of 2024-T3 aluminum alloy under narrow band random acoustic loading, have been conducted at NAL, and data of rms stress vs. number of cycles to failure were obtained. Fig. 15 shows estimated acoustic S-N curve and the experimental results. In this figure, the results for bond-riveted panel lie on the same S-N curve as riveted panel, which was reported in ICAF Doc. No. 800.

Also, a program of work on acoustic fatigue of fiber reinforced plastics panel specimen is now in progress at NAL.

3. THE THIRD RESEARCH CENTER, T.R.D.I.*, JAPAN DEFENCE AGENCY

3. 1 Full Scale Fatigue Test of the C-1 Twin-Turbofan Military Transport

The full scale fatigue test of the C-1 transport was finished at the end of November 1974.

The number of the total damages, which included unimportant damages such as cupping of rivets and loosing of screws, was 462 as shown in Fig. 16. Most of the damages were initiated and propagated by the cabin pressure loads, the landing loads such as spin-up and spring-back, and taxiing loads such as braking, turning and pivoting.

The most important damage which determined the service life of the C-1 airplane was discovered on the trunnion fitting of the left main landing grear at 53,853 flights. The location and the detail of this damage are shown in Fig. 17 and Fig. 18. According to the fractography of the fracture surface, it is concluded that this damage is initiated at A and B shown in Fig. 18, in which the cracks meet at almost right angles.

Since cracks are initiated and propagated in the normal direction of the principal stresses, it is thought that the cracks were caused by two different principal stresses which arose from the cyclic shear loads. These alternative shear loads were brought by the alternative longitudinal forces which acted on the outer lag of this trunnion fitting and twisted the I-section of this fitting.

The corner radius of this I-section turned out to be too small compared with the flange thickness. Therefore, the corner radius of 5 mm as shown in Fig. 18, section A-A, was changed to 15 mm for the production airplane. Accordingly the stress concentration factor of 8.75 was reduced to 3.60.

All other damaged parts, except items which would not have influence on the service life of the C-1 transport airplane, were modified. (*T.R.D.I.; the Technical Research and Development Institute)

3. 2 Full Scale Fatigue Test of the PS-1 4-Turboprop STOL Flying Boat

STOL flying boat PS-1 was developed as an ASW* seaplane possessing dunking sonar and a capability to operate in rough sea.

PS-1 has been delivered to MSDF** since 1968 and is now under production.

The full scale fatigue test of PS-1 STOL flying boat was conducted from July to December in 1975 by random repeated loads corresponding to more than 20,000 take off and landings on the water, at the Third Research Center.

The arrangement of 122 hydraulic actuators for external loads is shown in Fig. 19(a).

In addition to the flight loads of conventional airplane, the hull structure of the seaplane was repeatedly loaded corresponding to take off and landings on the water by the specially constructed loading cradle with hydraulic actuators connected to loading pads on the hull bottom as shown in Fig. 19(b). The load spectrum was decided according to the U.S.A. military specification. The programmed load spectrum was designed by flight-by-flight loads with the random external loads.

Besides, two kinds of hull bottom panels representing the keel area and chain area near the step of PS-1, were tested by air pressure simulating random water loads according to MIL-A-8867. The illustration of this test is shown in Fig. 20.

(*ASW; Anti-Submarine Warfare, **MSDF; Maritime Self Defence Force)

3. 3 Landing Gear Fatigue Test of the US-1 4-Turboprop STOL Amhibious Flying Boat

US-1 is an amhibious version of the PS-1 STOL flying boat which is now under production.

The fatigue test of main landing gears and their fittings of US-1 amphibious seaplane was conducted from December in 1975 to January in 1976 by random repeated loads corresponding to about 20,000 take off and landings at the Third Research Center.

The frequencies of the loads were decided according to the U.S.A. military specification.

4. FUJI HEAVY INDUSTRIES, LTD., AIRCRAFT DIVISION

4.1 Full Scale Safe Life Test of the Model 700

Full scale safe life testing of the Model 700 is underway at the Fuji Aircraft Division in Utsunomiya, Japan. The Model 700, which is being developed by Fuji and The General Aviation Division of Rockwell International, is a pressurized, twin engine general usage airplane, designed for certification under the N category of JCAB airworthiness regulation and FAR Part 23.

The fatigue test article consists of both left and right wing structures, the fuselage structure and the tail structure without control surfaces, as shown in Fig. 21. The test article is free floated and loaded with twelve hydraulic jacks and one pressurization air source. Flight-by-flight load sequence with five types of programmed flight cycles, as shown in Fig. 22, was adopted in order to account for the combined effects of pressurization load, flight load and ground load.

To assure full cabin pressure load, the cabin compartment is pressurized using air pressure to the maximum cabin pressure setting plus the average external aerodynamic suction. The windshield is loaded, in addition to the air pressure mentioned above, with a whiffle system to account for the local peak of the aerodynamic suction.

Flight load and ground load spectra specified by FAA (AFS-120-73-2) were applied to determine the test load spectrum. A combined gust and maneuver load spectrum was designed by six load steps. As the calculated damage due to landing and taxiing load spectra themselves are negligibly smaller than the damage due to flight load spectrum, a taxiing load of 1.33g is applied once per flight in order to account for the gound-air-ground effect.

Fig. 22 shows the loading pattern of cabin pressure load, flight load and ground load. One flight cycle is represented as 1.1 flight hours and five patterns of programmed load are adopted for flight load. The severest pattern of flight load (−0.64g to 3.0g) appears once every 240 flights, and, as a convenience, a set of 240 flight cycles (264 flight hours) is called one "block".

The test setup is shown in Fig. 21 schematically. The flight load and inertia load during taxiing are distributed over the wing, including the leading edge section, using tension pads and whiffle systems. The engine inertia load and the main landing gear load are applied by hydraulic jacks through dummy engines and dummy landing gears. The horizontal tail load, which is offset from the center line to introduce rolling moment in the inclined gust condition, is applied by a hydraulic jack and batter boards. The fuselage loads were determined mainly so as to balance with the wing and horizontal tail loads, which resulted to cover the critical fuselage bending moment in the symmetrical gust condition.

The testing time for one flight cycle is about 100 seconds which is carefully determined so that the oscillatory acceleration of the dead weights of the test setup would not affect the test load. The scatter factor to determine safe life from the tested life is 4.0 according to AFS-120-73-2.

5. MITSUBISHI HEAVY INDUSTRIES, LTD., AIRCRAFT WORKS

5.1 Fatigue Life Estimation

Though Miner's rule is widely used in the calculation of the fatigue life of airplane structures, there are many problems in its applicability. In the portion of stress concentration, the residual stress that is induced by large stress and partial yielding, affects its fatigue life significantly. So, it is necessary to take into account the residual stress, and methods for this purpose are proposed, for example, Smith's method and Impellizzeri's method.

We studied these methods for improving its accuracy and extending its usability, following two modifications for Impellizzeri's method were made.

(1) The stress in the area of stress concentration which was used in calculating the fatigue life was accounted from the residual stress predetermined by measuring on test pieces with various stress concentrations.

(2) The fatigue life was determined by using constant life fatigue diagrams, provided that the residual stress has equal effect to average stress on fatigue life.

By above mentioned modifications of the method, we obtained high accuracy and wider usefulness on fatigue life estimation.

5.2 Evaluation of Defects of Airplane Forging Materials

Evaluation of forging defects of Ti-6Al-4V and aluminum alloys by using the linear fracture mechanics were studied. Provided that forging defects were equivalent to cracks, for the purpose of estimating the fatigue life of defected parts, number of stress cycles accumulated before the crack attained to critical size which depends on the fracture toughness value, was calculated using the rate of fatigue crack propagation of the material. And also stress determined from threshold stress intensity and defects size was calculated as the fatigue limit of the defected part. These values agreed fairly well with experimentally determined fatigue life and fatigue limit of parts.

It was also found that the part through slit produced by electron-discharge machining simulates well real forging defects.

5.3 Quantitative Evaluation of Electron-Fractography of Fatigue Fracture Surface

For a quantitative evaluation of the fatigue fracture surface by electron fractography were performed on aluminum alloys. The spacing of striation which is characteristic pattern of fatigue fracture surface is linearly related to crack tip stress intensity factors (ΔK). But another parameter R, stress ratio, also affects the spacing of striation, so we cannot determine the stress condition definitely by measurement of spacing, namely striation spacing P is $P = f(\Delta K, R)$. To determine ΔK and R simultaneously, another parameter which is quantitatively related with ΔK and R is needed.

We, noting the depth of plastically deformed layer developing along surface of fatigue fracture, tried to estimate the stress condition by measuring the depth of this layer by means of X-ray diffraction method. Depth of this layer δ was determined experimentally, as $\delta = g(\Delta K, R)$. So, by measuring P and δ, ΔK and R were estimated as the intersect of function $f(\Delta K, R) = P$ and $g(\Delta K, R) = \delta$.

5.4 Crack Propagation and Non-Propagating Limit

Crack propagation in structural part under the condition of its practical use is different from crack propagation subjected to constant repeated stress. Generally, crack propagation rate after larger stress decreases from its original rate of propagation, and non-propagating limit increases from its crack propagating threshold stress intensity value.

Therefore, to calculate the crack propagation under practical condition, it is fundamentally necessary to know about the crack propagation characteristics under two step stress condition. We studied this problems and the following results were obtained.

Under two step repeated stress, when the second stress level is higher than the first one, crack propagation rate does not change essentially from its original one. On the other hand, when the second stress level is lower than the first one, crack propagation rate is significantly retarded and this retardation is approximately explained by Wheeler's model which proposes to apply the retardation effect of single overload.

Next, non-propagating limit ΔKe, represented by stress intensity range, is also linearly related to the first step condition ΔKi, represented by stress intensity.

Using above mentioned results, we can estimate the crack propagation under practical stress conditions.

5.5 Fatigue Strength of Structural Elements

Fatigue tests were performed on various structural elements for obtaining the design data and improving the fatigue property. These were fatigue tests of lugs loaded sidely and various types of mechanical joints, for example, joints with bonded doublers, CFRP joints and joints of honeycomb sandwich structures.

5.6 Effects of Plating on Fatigue Strength of Low Alloy Ultra-High Strength Steels for Airplane Landing Equipments

Effects of Cr, Ni and Ti-Cd plating on fatigue strength of low alloy steel (tensile strength 200kg/mm^2) were studied. Fatigue limits decrease by plating, for example, to 30% of original material in Cr plating to 40% in Ni plating, and to 95% in Ti-Cd plating. By applying the shot peenings before plating,

fatigue strength recovers completely.

5.7 Fatigue Strength of Electron Beam Welded and Diffusion Bonded Aluminum Alloy and Titanium Alloy Parts

To evaluate strength of large fittings produced by electron beam welding and diffusion bonding, fatigue tests were made for 7075-T6 and Ti-6Al-4V alloys.

In the case of electron beam welded 7075-T6 alloys, same fatigue strength to its original alloys was obtained, provided that solution treatment and aging were performed again after welding.

For Ti-6Al-4V alloys, electron beam welded and diffusion bonded areas have equal or better fatigue properties than its original material's properties.

6. KAWASAKI HEAVY INDUSTRIES, LTD., AIRCRAFT GROUP

6.1 Fatigue Evaluation of Glass Fiber Reinforced Plastics

For the purpose of obtaining the basic design data for helicopter components, a fatigue evaluation was conducted on GFRP specimens that were fabricated by Kawasaki Heavy Industries.

Materials were Asahi Kasei PPG 1062 glass roving (13μm diameter fiber), Asahi Kasei PPG 713 glass roving (9μm diameter fiber) and Shell Epicote 827 epoxy. Each specimen was fabricated with 0° fiber orientation and its minimum cross section was 3mm X 2mm or 4mm X 3mm. Fatigue tests were conducted at a frequency of either 10 Hz or 33 Hz using two types of testing machines under the stress ratio of R = 0 at room temperature.

Fatigue tests under two kinds of two-stress-level loading sequence were also conducted which were considered to simulate the operating loads of helicopter rotor. These two kinds of loading sequence were (A) $\sigma_1 = 74\,kg/mm^2$ 500 cycles, $\sigma_2 = 64\,kg/mm^2$ 6,000 cycles and (B) $\sigma_1 = 74\,kg/mm^2$ 500 cycles, $\sigma_3 = 55\,kg/mm^2$ 32,000 cycles. Test results are shown in Fig. 23, where $\bar{N}_f$ is the arithmetic mean of the number of cycles to failure at each stress level (σ_1, σ_2 and σ_3) for all lots. N_f is the arithmetic mean of the number of cycles to failure at each stress level for each lot.

The results of this evaluation program are as follows;

(1) Static shear strength and fatigue tensile strength have an obvious correlation with V_f (fiber volume fraction)

(2) The fatigue strength of the specimen with 9μm diameter fiber is higher than that of the specimen with 13μm diameter fiber for up to 10^6 cycles of loading, but both of the specimens have a comparative fatigue strength for $10^6 \sim 10^7$ cycles.

(3) Loading frequencies of 10 Hz and 33 Hz have no influence on fatigue strength.

(4) The test specimen with 0° fiber orientation did not undergo any decrease in its modulus of elasticity during the tension-tension fatigue test.

(5) The cumulative linear damage theory is reasonably valid under two-stress-level loading for those GFRP specimens.

6.2 The Effect of Pre-Load for Pressurized Cabin

According to MIL-A-8867A and BCAR D-3, the pre-load applied prior to pressurized flight is specified as the 1.33 times maximum operating pressure. However, it is well known that the fatigue life of pressurized cabin structure is increased by this load. In order to obtain the qualitative and quantitative data on the effect of pre-load, the test and analysis are carried out, changing the value of pre-load, the interval of periodic pre-load in cyclic load and the cyclic load level.

Two types of 2024C-T3 aluminum alloy specimens (Fig. 24) which are the typical fuselage skin splices are used in this test. As three specimens are tested for one item, their geometric mean is taken as the test result. From the static test of Type 1, it is found out that the ultimate strength is about $38\,kg/mm^2$. Fig. 25 shows the relationship between the fatigue life ratio $\bar{N}_p/\bar{N}_o$ = (fatigue life with pre-load) / (fatigue life without pre-load) and the pre-load ratio $P_{pre}/P_{fatigue}$ = (pre-load) / (cyclic load). On the other hand, the effect of periodic pre-load is shown in Fig. 26 in which $\bar{N}_{\Delta n}$ is the fatigue life for the interval Δn of periodic pre-load. From these test results, it is pointed out that there are the most effective value of pre-load and the optimal interval of periodic pre-load. In detail, the most effective value of Type 1 is about 80% of ultimate strength without being affected by the cyclic load level, and also it is clear that the pre-load which is the 1.33 times maximum operating pressure increases the fatigue life. The maximum

value $\bar{N}_p/\bar{N}_o$ of Type 1 is larger than that of Type 2. The reason why such result is obtained is regarded that the stress concentration of the latter is more remarkable than that of the former. As to the effect of periodic pre-load, it is shown that the optimal interval is about one third of $\bar{N}_o$. As there is no adequate method to estimate the fatigue life considering the effect of excessive tensile load, the modified Impellizzeri's method which takes account of the Bauschinger effect is utilized. Although the estimated lives are shown in Fig. 25, these are generally less than the test results. In other words, it should be noted that the effect of pre-load is more significant than the calculation in this test.

7. ACKNOWLEDGEMENT

The authors wish to express their sincerest gratitude for Dr. L.E. Jarfall and Dr. O. Buxbaum, in cordially inviting Japan to the 15th ICAF Meeting as a guest and granting a precious opportunity to review the recent aeronautical fatigue investigation in Japan. They also earnestly desire to be able to have such occasion in the future in order to exchange useful informations on aeronautical fatigue.

Finally, they greatly appreciate the cooperation and assistance of Prof. T. Yokobori and other members of Sixth Sub-Committee on Aeronautical Fatigue of the Japan Society for Promotion of Science, and Messrs. K. Ono, T. Sotozaki and S. Ito of First Airframe Division, NAL, in preparing the manuscript of this review.

8. REFERENCES

ICAF Doc. No.

823) T. Kamiyama; Scatter Factor for Fatigue Life of Civil Aircraft Structure. Reliability Approach in Structural Engineering (1975) Maruzen Co., Ltd., Tokyo.

824) T. Endo, K. Mitsunaga, K. Takahashi, K. Kobayashi and M. Matsuishi; Damage Evaluation of Metals for Random or Varying Loading – Three Aspects of Rain Flow Method –, Proceedings of the 1974 Symposium on Mechanical Behavior of Materials, Vol. 1, Mechanical Behavior of Materials.

825) T. Endo, K. Kobayashi, K. Mitsunaga and N. Sugimura; Numerical Comparison of the Cyclic Count Methods for Fatigue Damage Evaluation, and Plastic-Strain Damping Energy of Metals under Random Loading. 1975 Joint JSME-ASME Applied Mechanics Western Conference, 75-AM JSME A-17.

826) T. Yoshimura and T. Yokobori; Fatigue Reliability under Random Loadings. Reports of The Institute for Strength and Fracture of Materials, Tohoku Univ. Vol. 3 No. 2, Dec. (1967).

827) T. Yokobori, M. Ichikawa and H. Kawamoto; Fatigue Reliability under Random Loadings. Reports of The Research Institute for Strength and Fracture of Materials, Tohoku Univ. Vol. 8 No. 2, Dec. (1972).

828) T. Yokobori, M. Ichikawa and F. Fujita; A Stochastic Theory of Fracture of Solids Containing a Small Number of Macroscopic Defects. Reports of The Research Institute for Strength and Fracture of Materials, Tohoku Univ. Vol. 10 No. 1, Nov. (1974).

829) T. Yokobori and M. Ichikawa; Nonlinear Cumulative Damage Law for Time-Dependent Fracture Based on Stochastic Approach. Reports of The Research Institute for Strength and Fracture of Materials, Tohoku Univ. Vol. 10 No. 1, Nov. (1974).

830) Y. Sawaki and T. Yokobori; A Stochastic Theory Approach to Fracture of Solids Combining Microscopic and Macroscopic Variables. Reports of The Institute for Strength and Fracture of Materials, Tohoku Univ. Vol. 9 No. 1, Nov. (1973).

877) M. Ichikawa, N. Tagawa and T. Yokobori: A Stochastic Theory of Fracture of Elastic Type in Fibre Reinforced Composite Materials. Reports of The Research Institute for Strength and Fracture of Materials, Tohoku Univ. Vol. 11 No. 2, Dec. (1975).

878) H. Nishitani and Y. Murakami; Stress Intensity Factors of an Elliptical Crack of a Semi-Elliptical Crack Subject to Tension. International Journal of Fracture, Vol. 10 No. 3, Sept. (1974).

879) Y. Murakami, H. Nishitani and S. Kusumoto; Notch Effect in Low-Cycle Fatigue (2nd Report; Effect of Stress Change and Mean Stress).

Bulletin of the JSME, Vol. 18 No. 119, May (1975).

880) S. Sumi; Spectacle Pattern Correlation Method for Measurement of Surface Structural Change Caused by Fatigue. Proceedings of the Nineteenth Japan Congress on Materials Research. The Society of Materials Science, Japan (1976).

881) K. Ohji, K. Ogura and Y. Ohkubo; Cyclic Analysis of a Propagating Crack and its Correlation with Fatigue Crack Growth. Engineering Fracture Mechanics, Vol. 7 (1975).

882) T. Nakagawa; Response Reliability due to Random Parameter. Japan-U.S. Joint Seminor on Reliability Approach in Structural Engineering, Maruzen Co., Ltd., Tokyo, Japan (1975).

883) S. Sorano, C. Hiwa and T. Nakagawa; Effect of Thermal Softening on Fatigue Life of Nylon-6. Proceedings of The Eighteenth Japan Congress on Materials Research, The Society of Materials Science, Kyoto, Japan (1975).

884) M. Kawamoto, H. Ishikawa, N. Inoue and Y. Yoshida; Fatigue Test Results and Fatigue Life Estimation on Hard Steel and Aluminum Alloy under Random Loads. Bulletin of the JSME, Vol. 18 No. 122, Aug. (1975).

885) K. Endo and M. Watanabe; Effect of Water Environmental on Fatigue Behavior of GRP. Bulletin of the JSME, Vol. 18 No. 119, May (1975).

886) K. Endo, K. Komai and Y. Watase; Cathodic Protection in Corrosion Fatigue of an Al-Zn-Mg Alloy. Proceedings of The Nineteenth Japan Congress on Materials Research, The Society of Materials Science, Kyoto, Japan (1976).

887) M. Kikukawa and M. Jono; Cumulative Damage and Behavior of Plastic Strain in High and Low Cycle Fatigue, Proceedings of The 1971 International Conference on Mechanical Behavior of Materials, Vol. 11, The Society of Materials Science, Japan (1972).

Table 1 Fatigue Test Results of 41 Groups (n = 3)

Group Number	Load Sequence	Failure			Z
		First	Second	Third	
1	A	46800	47800	87100	1.02
2	A	38400	39390	43100	1.03
3	B	333600	342000	460700	1.03
4	B	46100	47900	49000	1.04
5	B	203400	215000	229000	1.06
6	A	70400	74600	108600	1.06
7	B	224100	240600	269200	1.07
8	A	220300	236100	245500	1.07
9	A	24000	25800	29000	1.08
10	B	479200	530100	630800	1.11
11	B	196820	219410	234320	1.11
12	A	143900	164000	223100	1.14
13	B	107530	127320	147410	1.18
14	B	79800	97500	173600	1.22
15	B	23700	29000	29200	1.22
16	B	274600	335710	566430	1.22
17	A	239600	294300	330800	1.23
18	B	59800	74100	75200	1.24
19	B	221700	275600	362000	1.24
20	B	193000	245700	315800	1.27
21	B	102900	135200	305200	1.31
22	A	22400	29400	51500	1.31
23	A	66100	86600	95000	1.31
24	B	788110	1043470	1432420	1.32
25	A	33200	44800	61600	1.35
26	A	46100	62400	66500	1.35
27	B	16500	22600	24500	1.37
28	B	132900	182100	328000	1.37
29	A	126300	177000	232000	1.40
30	B	258510	372200	591110	1.44
31	B	272720	415200	455000	1.52
32	A	13500	22200	23400	1.64
33	B	193600	322500	368500	1.67
34	B	553000	985760	985760	1.78
35	A	35600	66800	74600	1.88
36	A	228200	452400	656500	1.98
37	A	85800	170300	248400	1.98
38	A	59400	119400	157000	2.01
39	B	82100	207400	246300	2.53
40	B	154300	391800	487100	2.54
41	B	84100	353000	369500	4.20

Load Sequence A:Const.Amp.,Zero-Ten.
B:Const.Amp.,Ten.-Ten.

Table 2 Values of α and ϵ for Each Material (Freudenthal)

Material		α		ϵ
		Short Life	Long Life	
Al Alloy		4.5	3.5	0.01
Ti Alloy		3.0	2.5	0.05
Steel	100-200 ksi	3.5	3.0	0.10
	200-300 ksi	2.5	2.0	

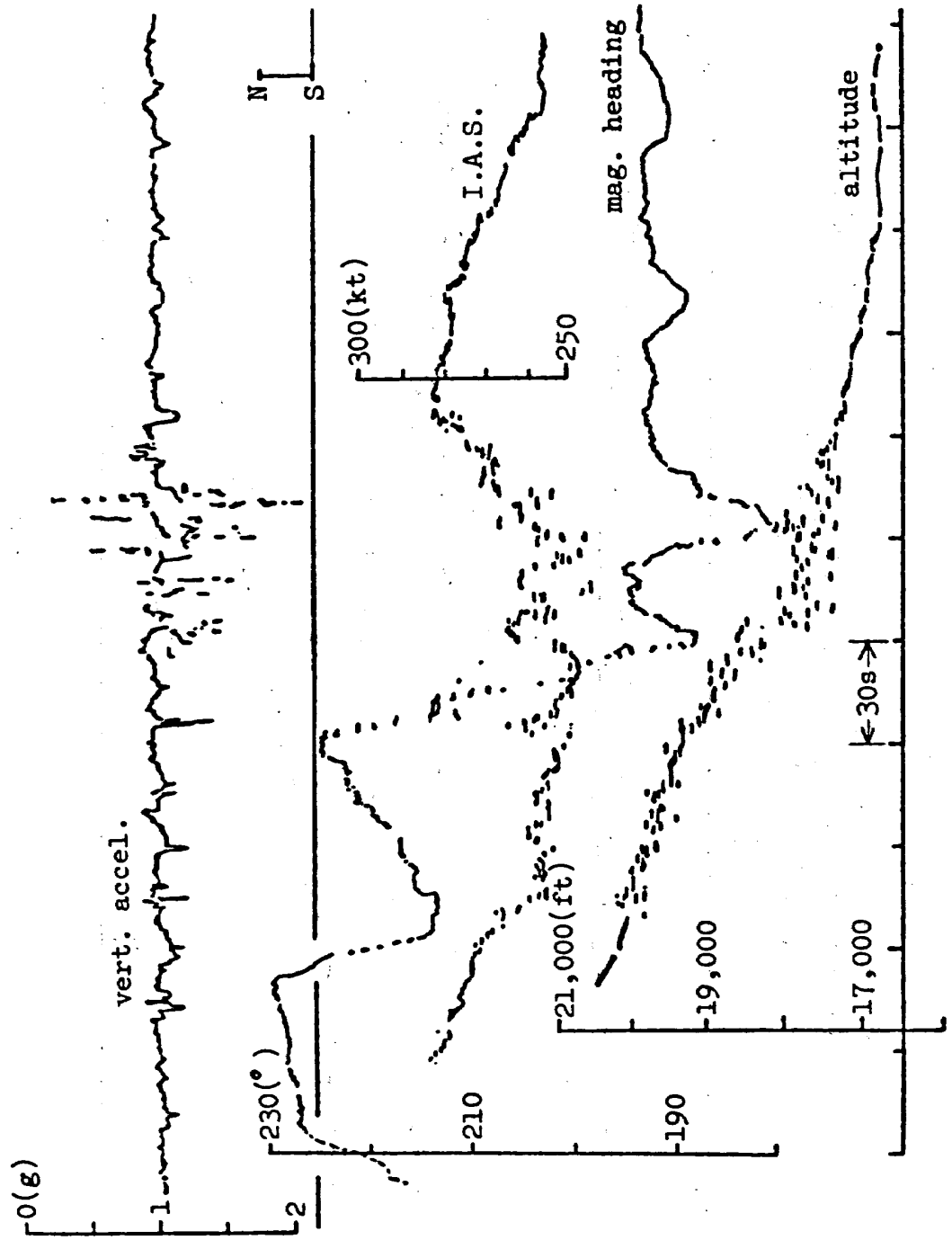

Fig. 1 Records of severe turbulence

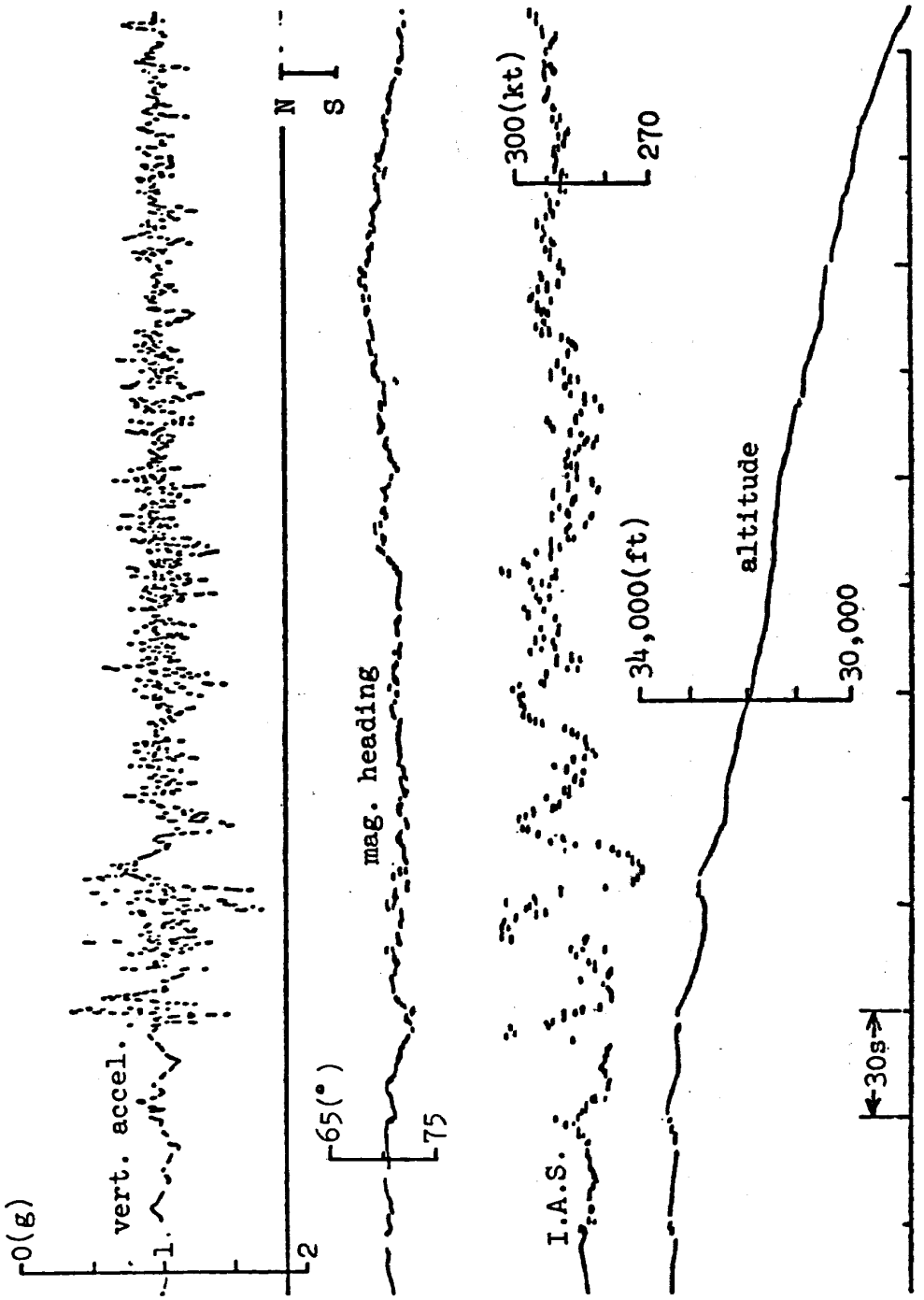

Fig. 2 Records of severe turbulence

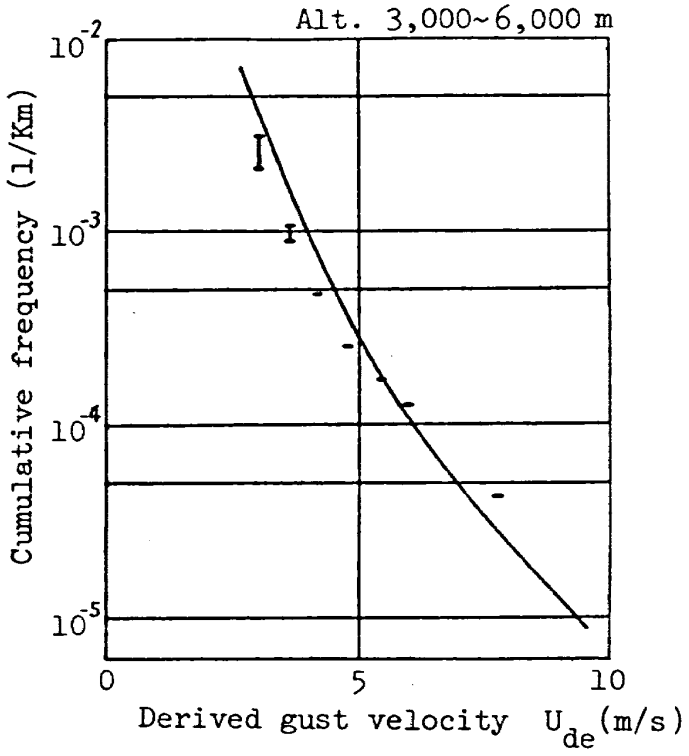

Fig. 3 Distribution of overall derived gust velocity for airplanes at 3,000 ~ 6,000 m altitudes

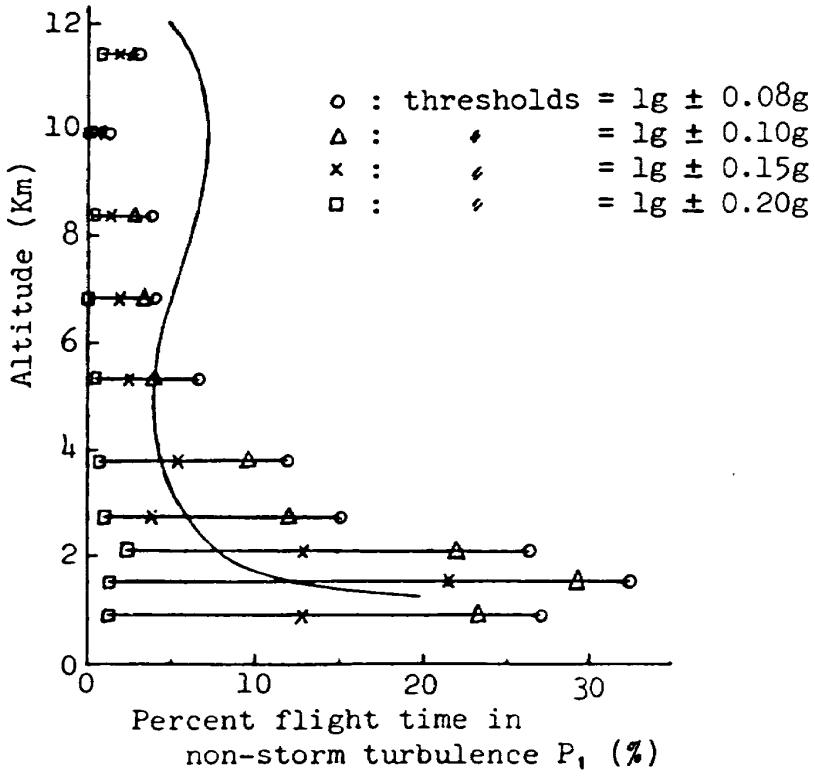

Fig. 4 Proportion of flight time in non-storm turbulence

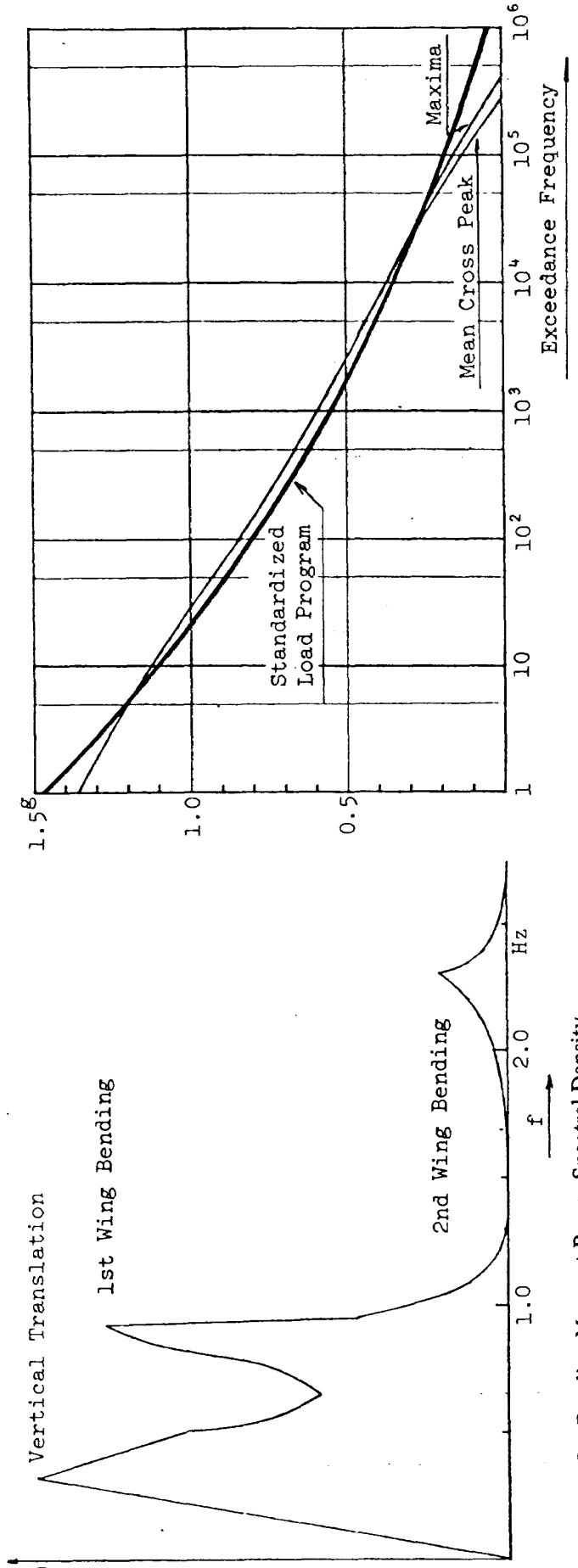

Fig. 5 Bending Moment Power Spectral Density of C-5A Wing Root (McDougal)

Fig. 7 Comparison of Exceedance Frequency for 2000 flights

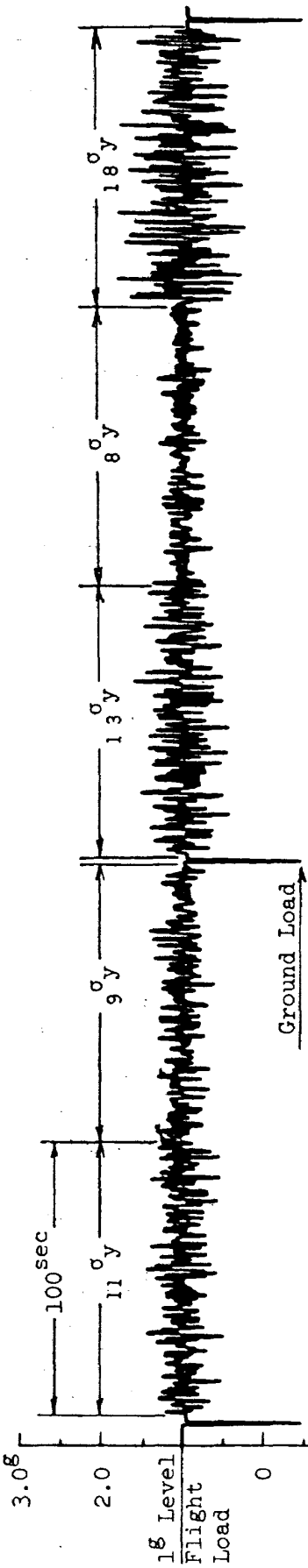

Fig. 6 Example of Flight-by-Flight Load

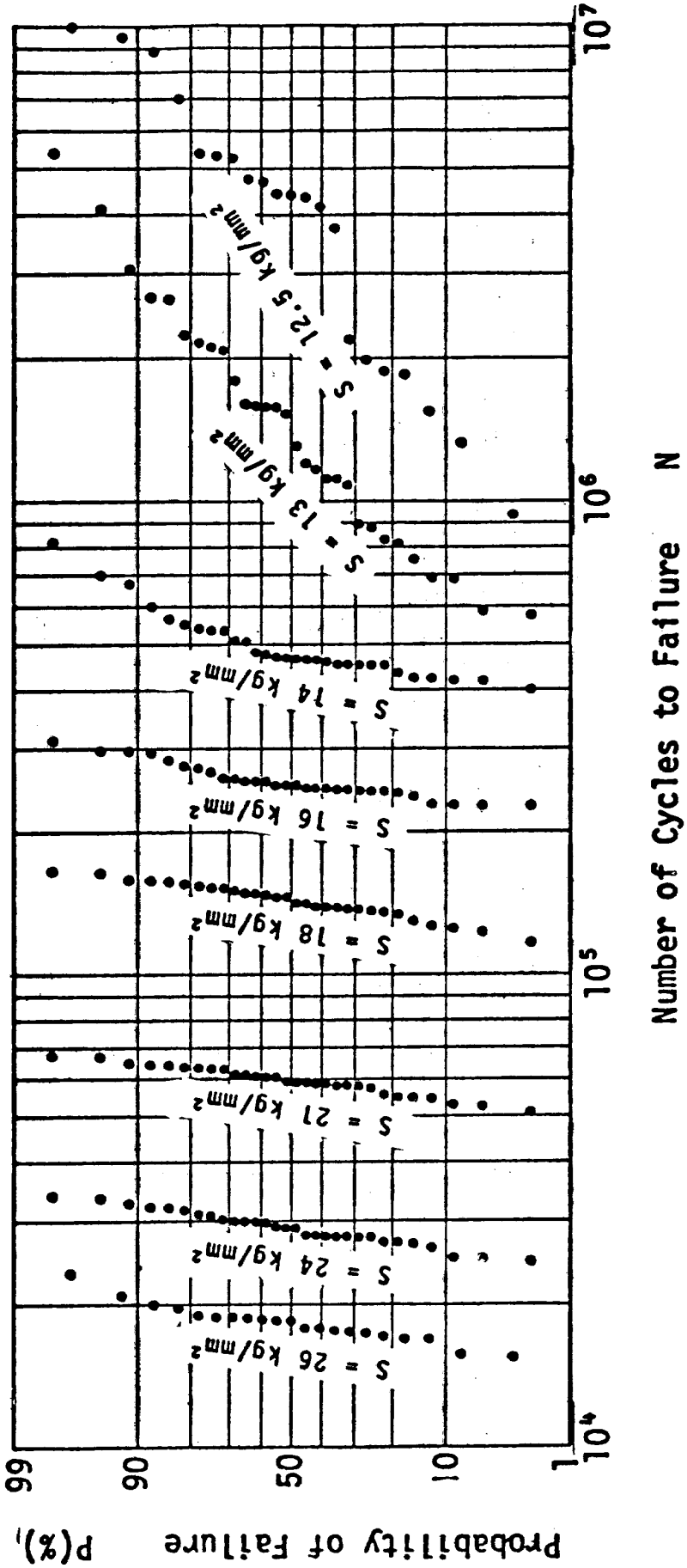

Fig. 8 Fatigue Life Distribution for $K_t = 2.54$

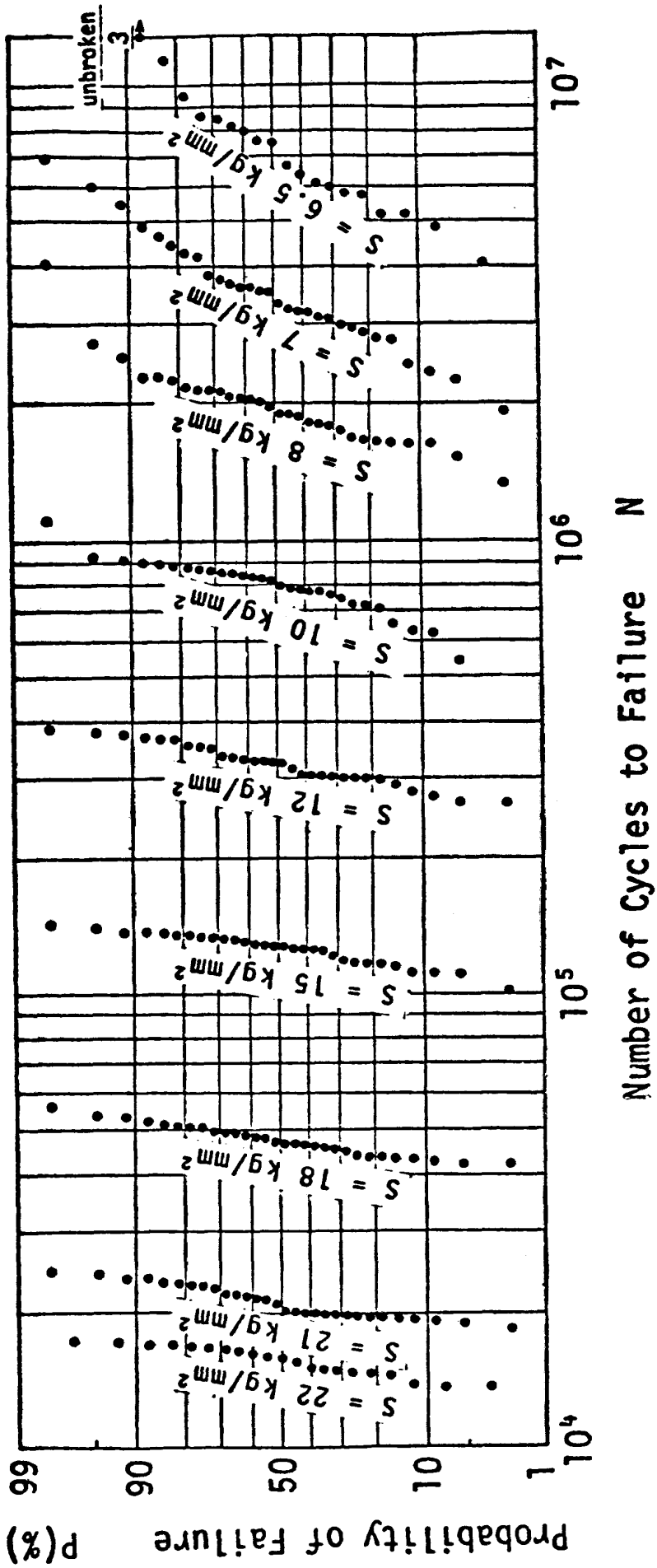

Fig. 9 Fatigue Life Distribution for $K_t = 8.25$

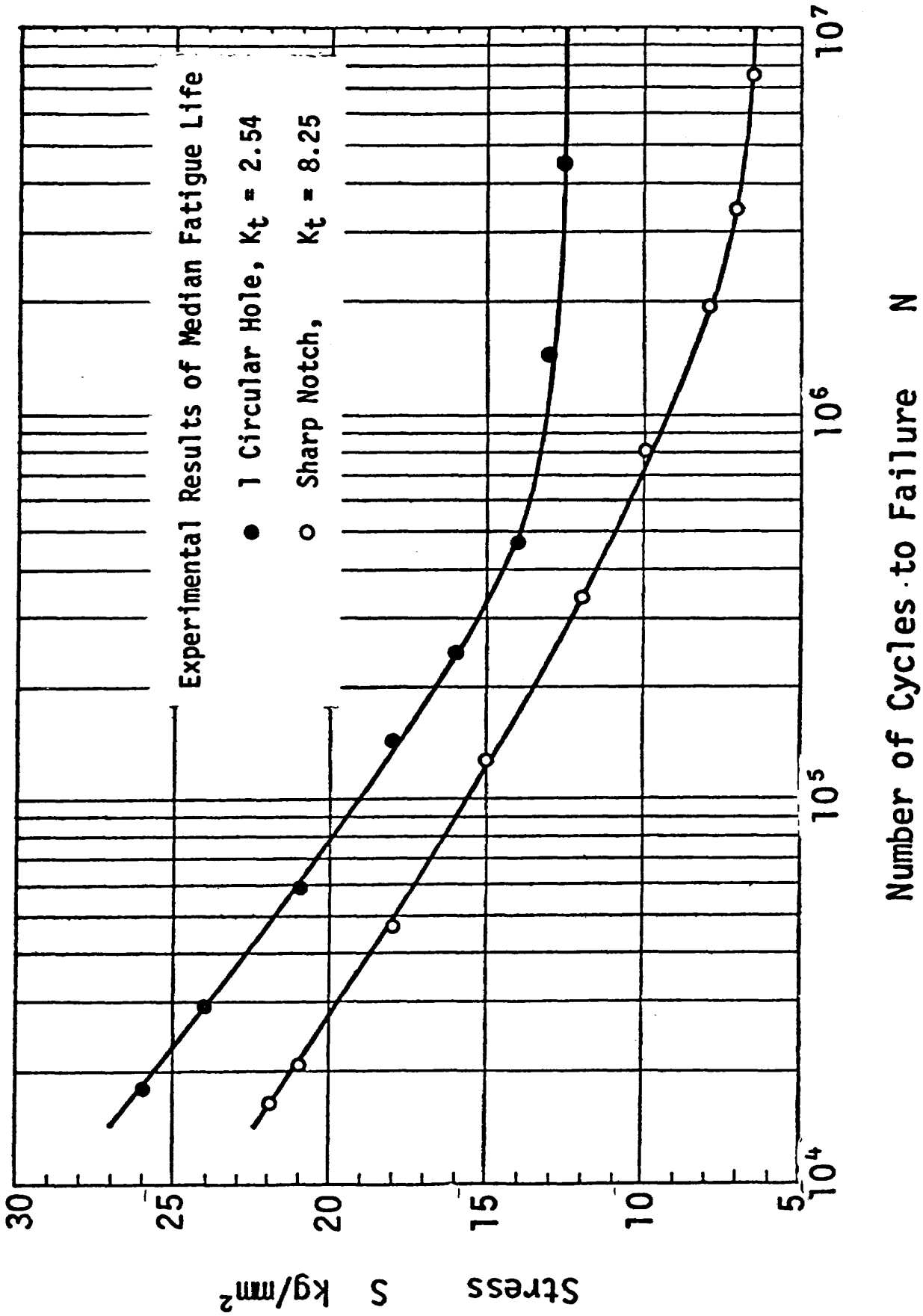

Fig. 10 S-N Curves for $K_t = 2.54$ and $K_t = 8.25$

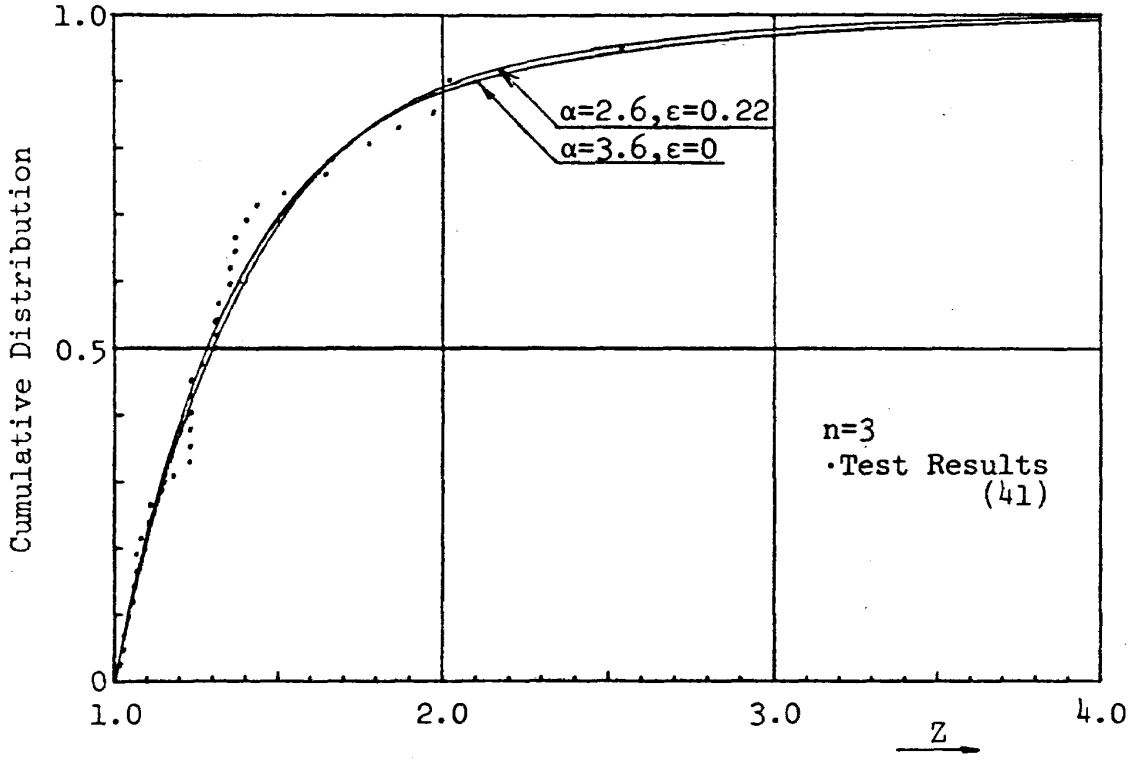

Fig. 11 Distribution of Random Variable Z

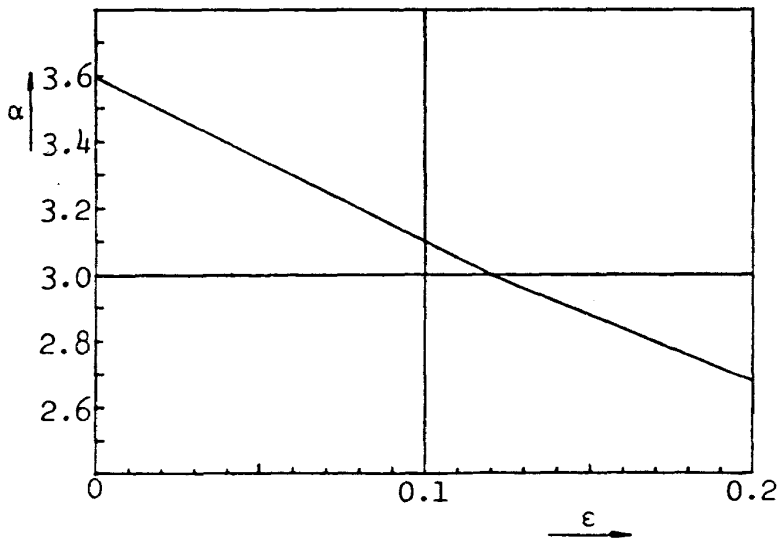

Fig. 12 Relation between α and ϵ

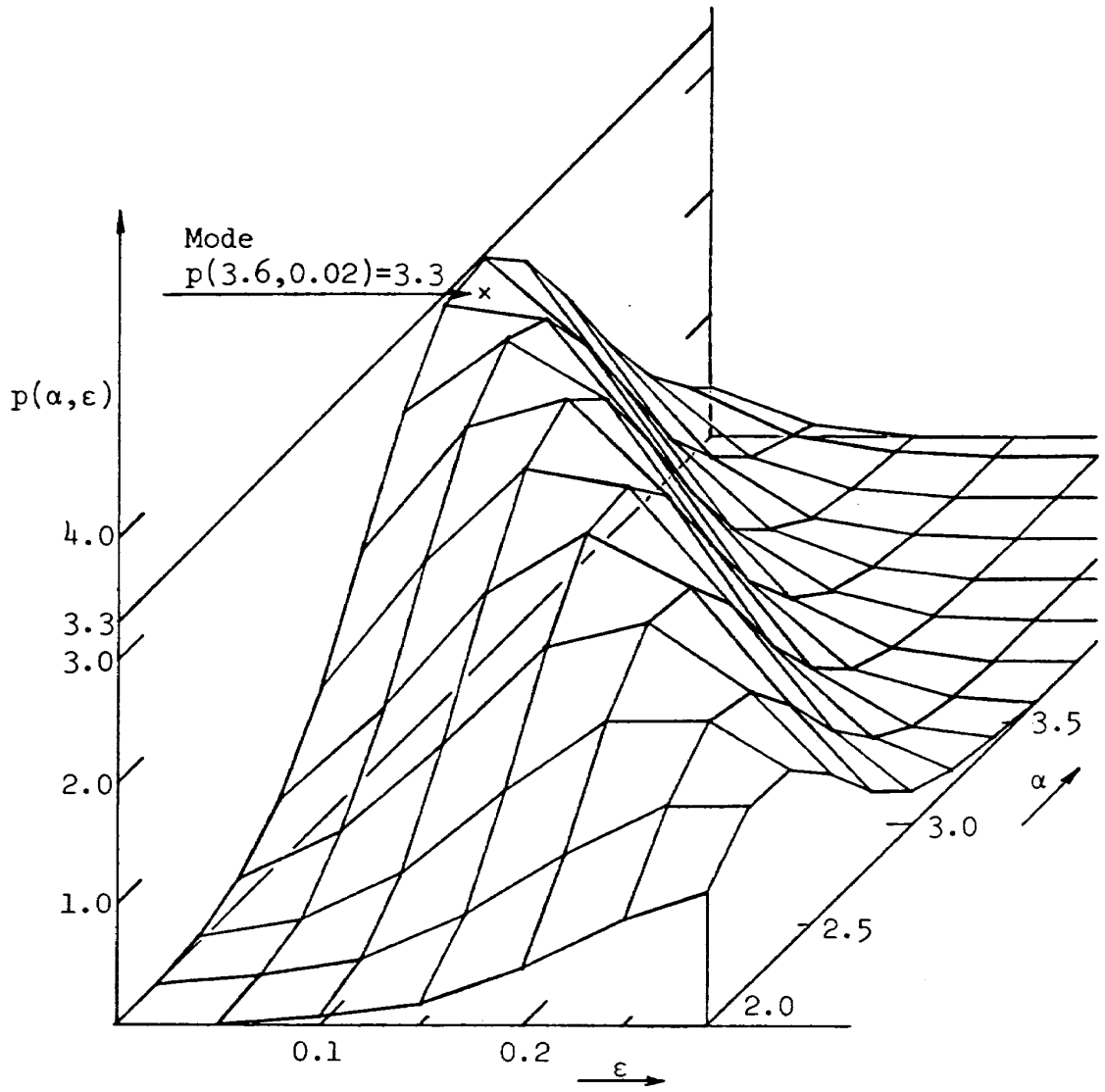

Fig. 13 Posterior Joint Probability

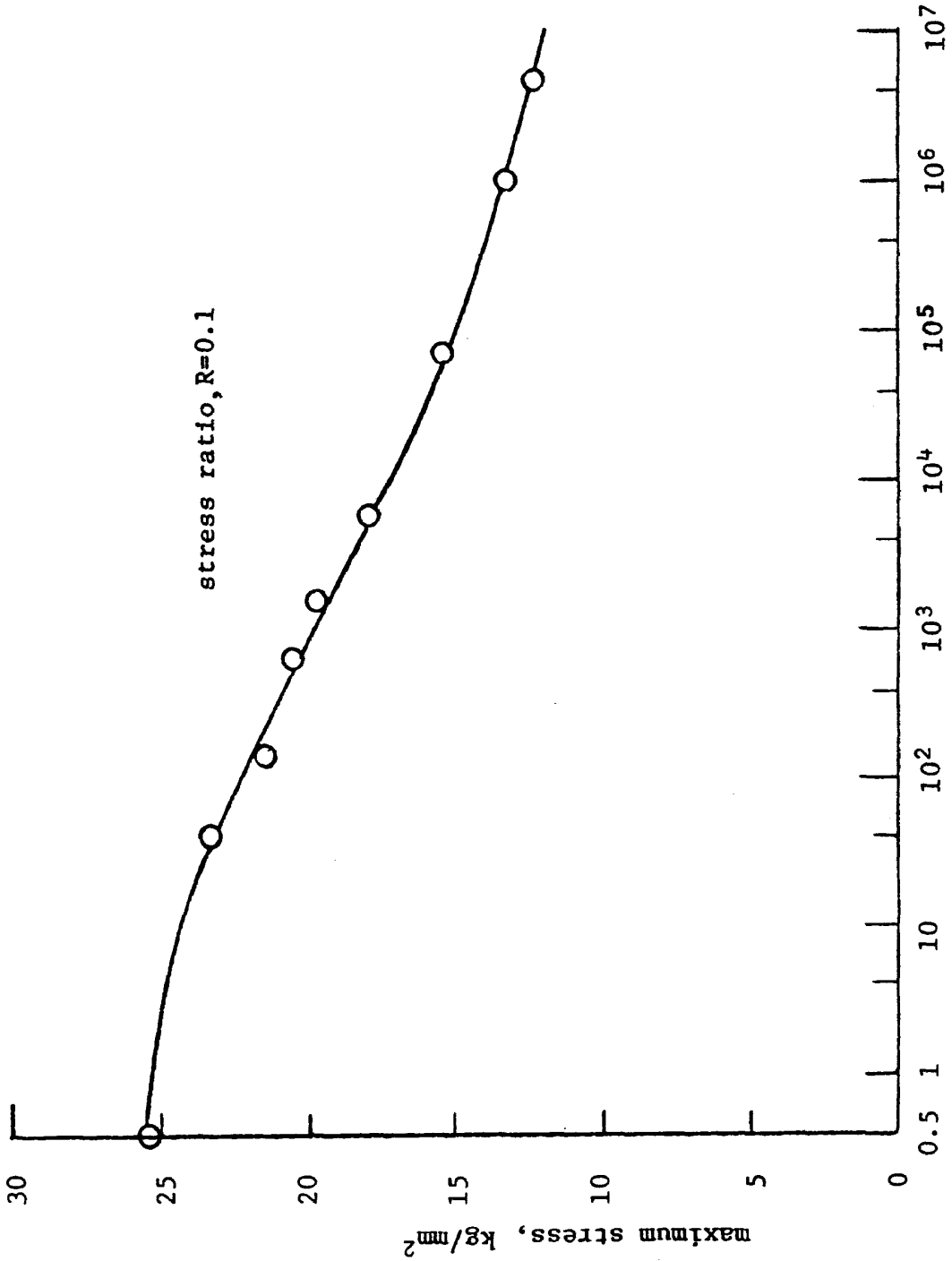

Fig. 14 S-N Curve for CFRP Aluminum Honeycomb Sandwich

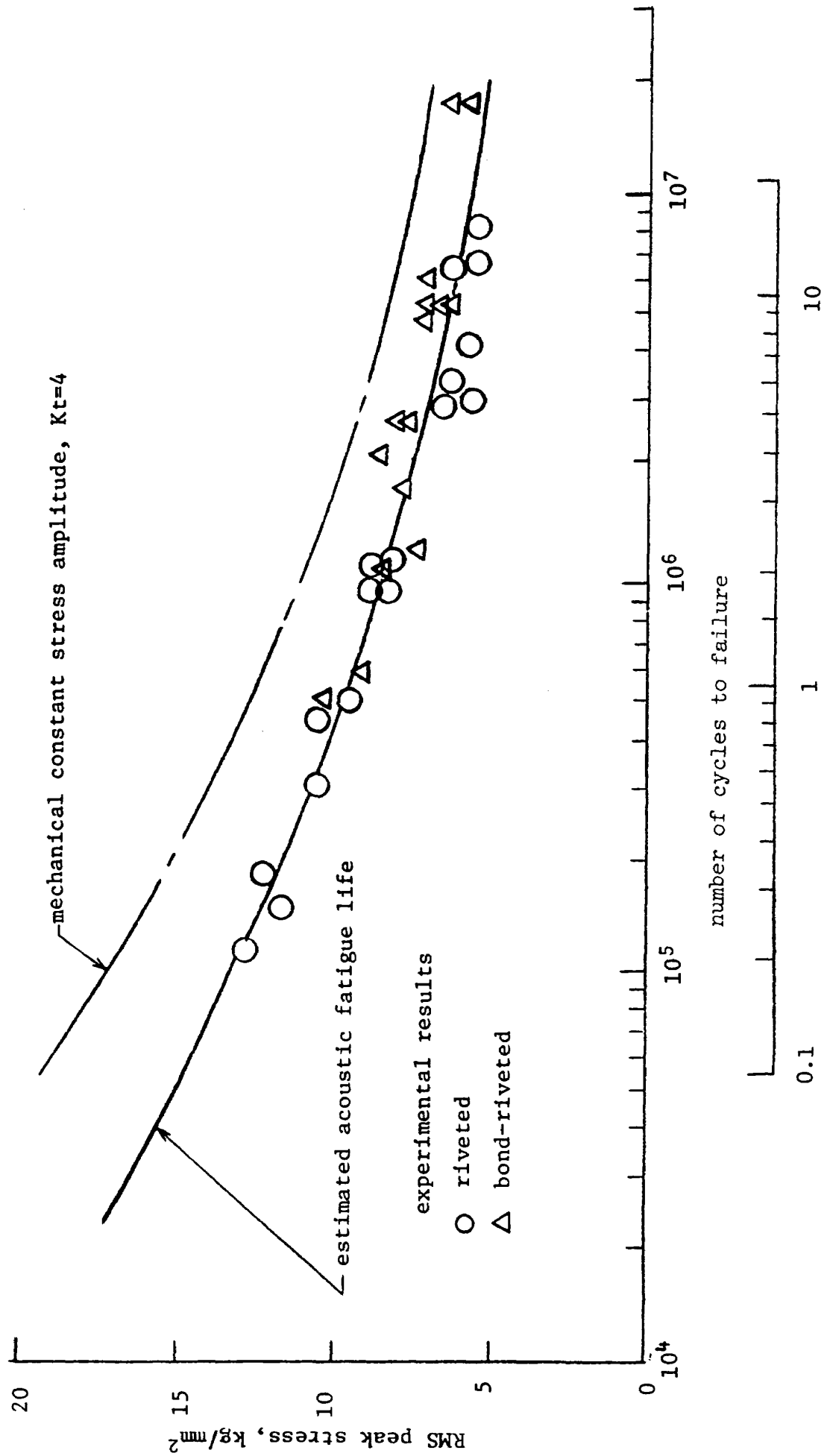

Fig. 15 Estimated Acoustic S-N Curve and Experimental Results

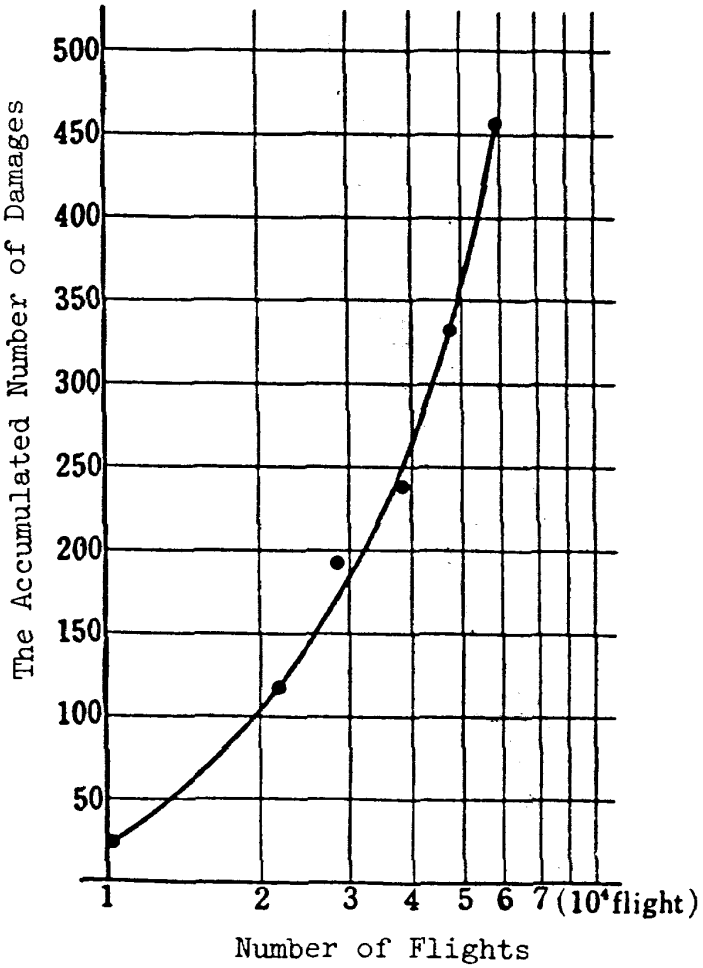

Fig. 16 The Accumulated Number of Damages of the C-1

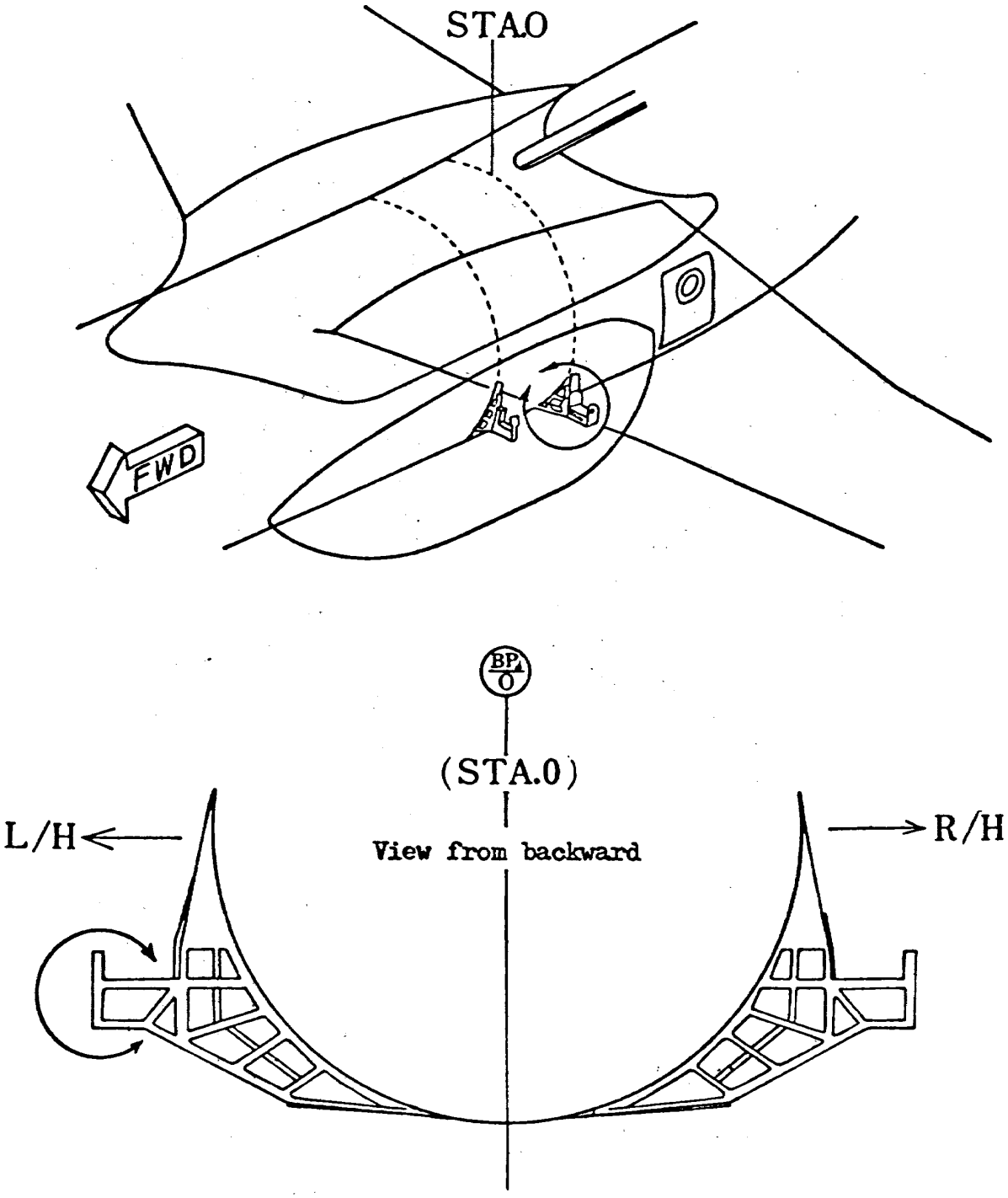

Fig. 17 The Location of the Damage

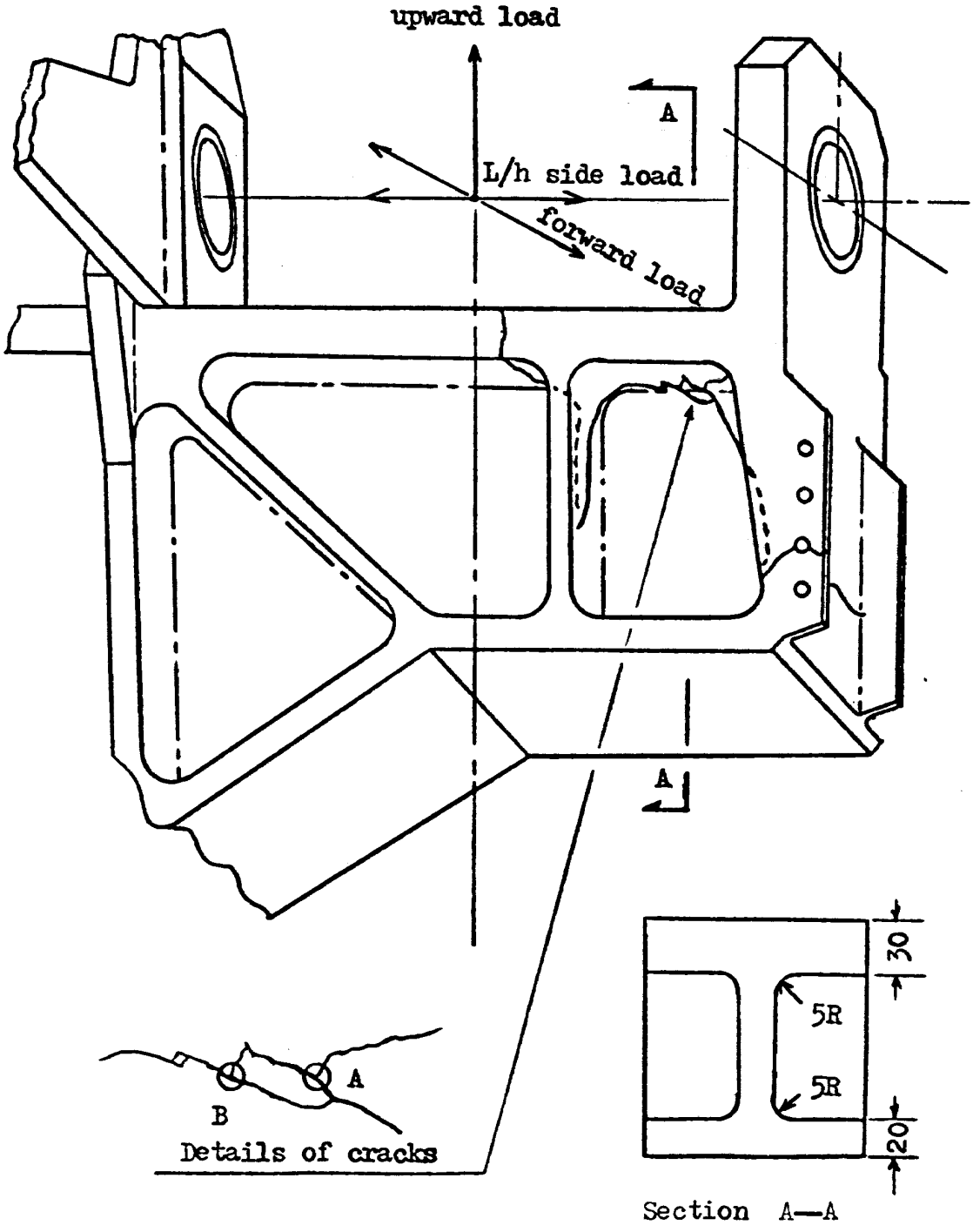

Fig. 18 A Schematic View of the Damage

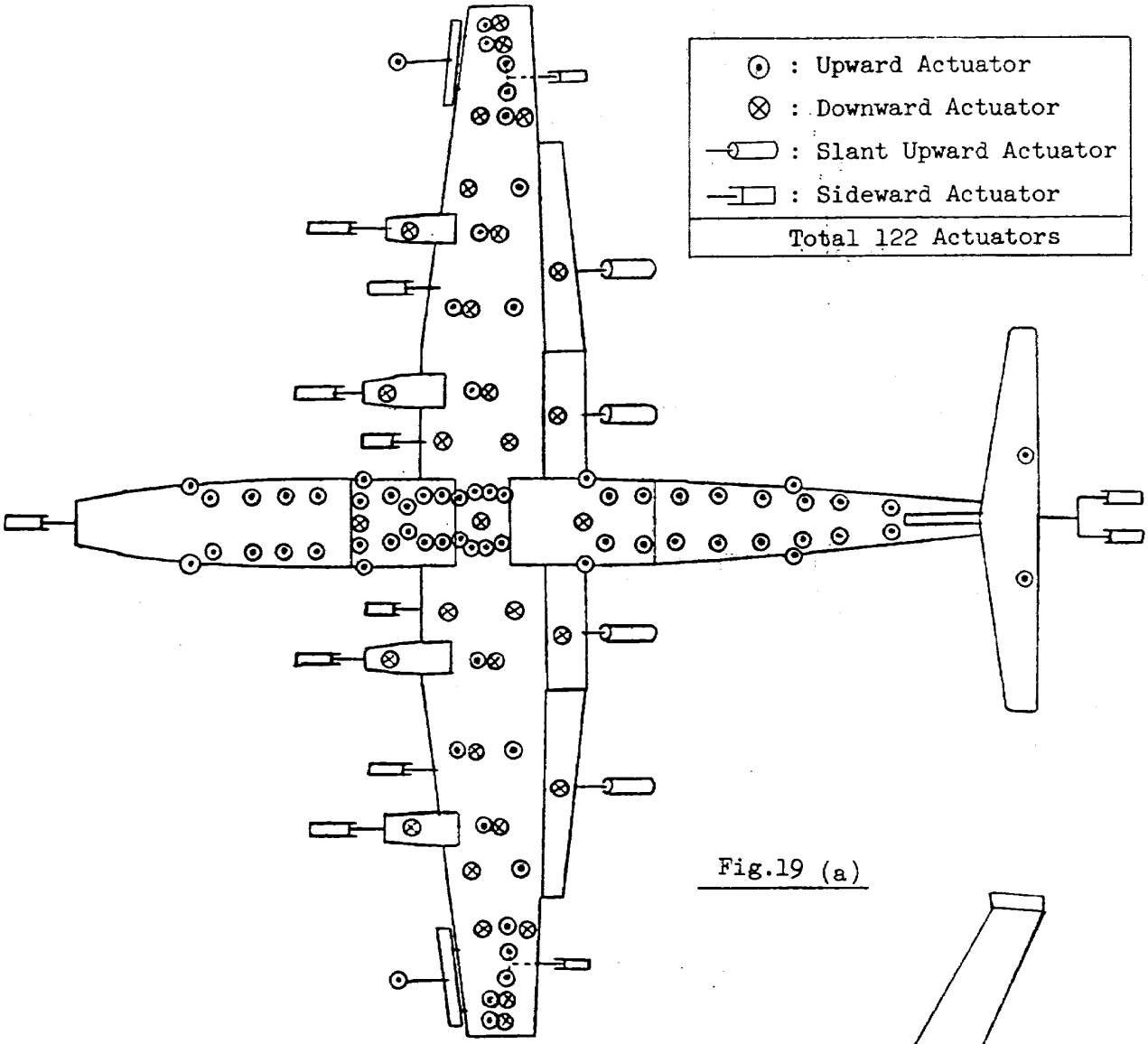

Fig.19 (a)

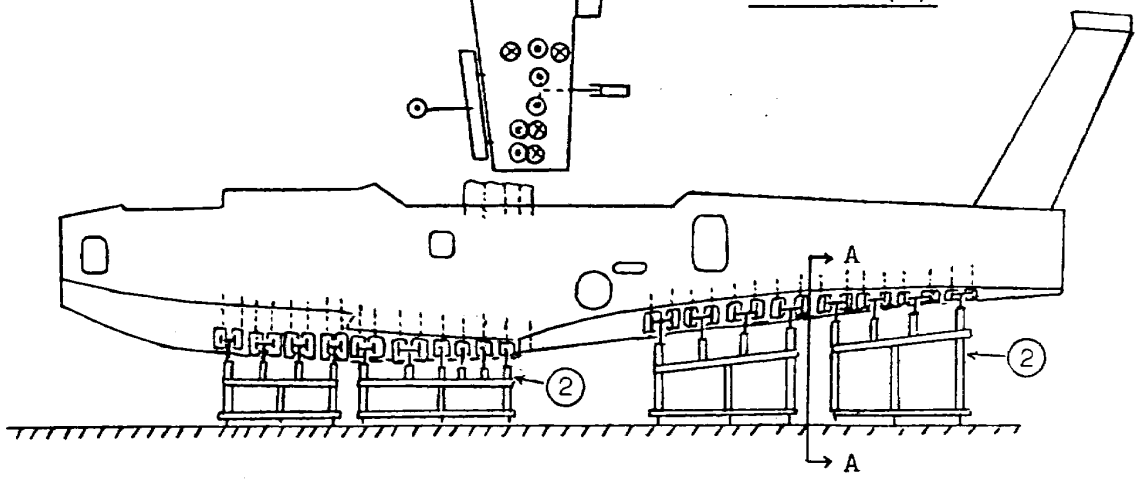

① : PS-1 Hull
② : Hull Loading Cradle
③ : Loading Pad with Rubber
④ : Hydraulic Actuator
⑤ : Load Cell

Fig.19 (b)

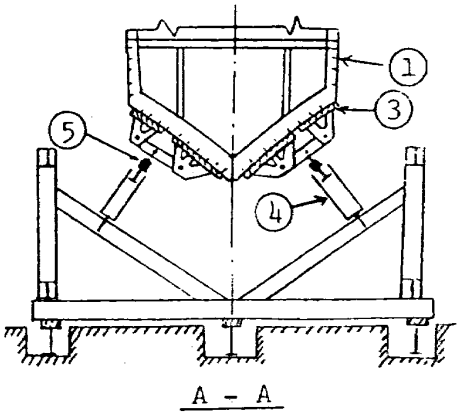

Fig. 19 Actuator Arrangement and Hull Loading Cradle of PS-1 Full Scale Fatigue Test

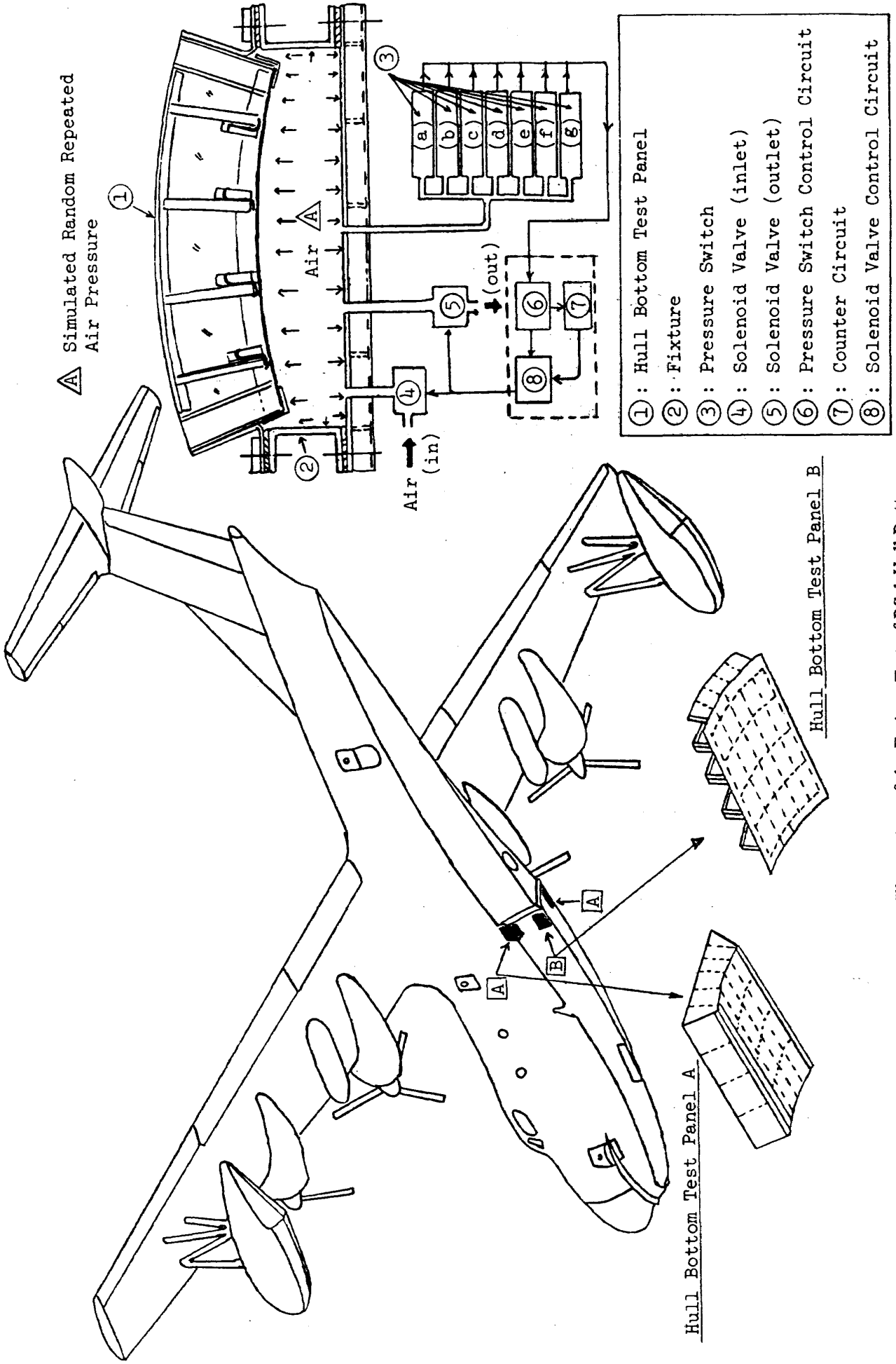

Fig. 20 Illustration of the Fatigue Test of PS-1 Hull Bottom

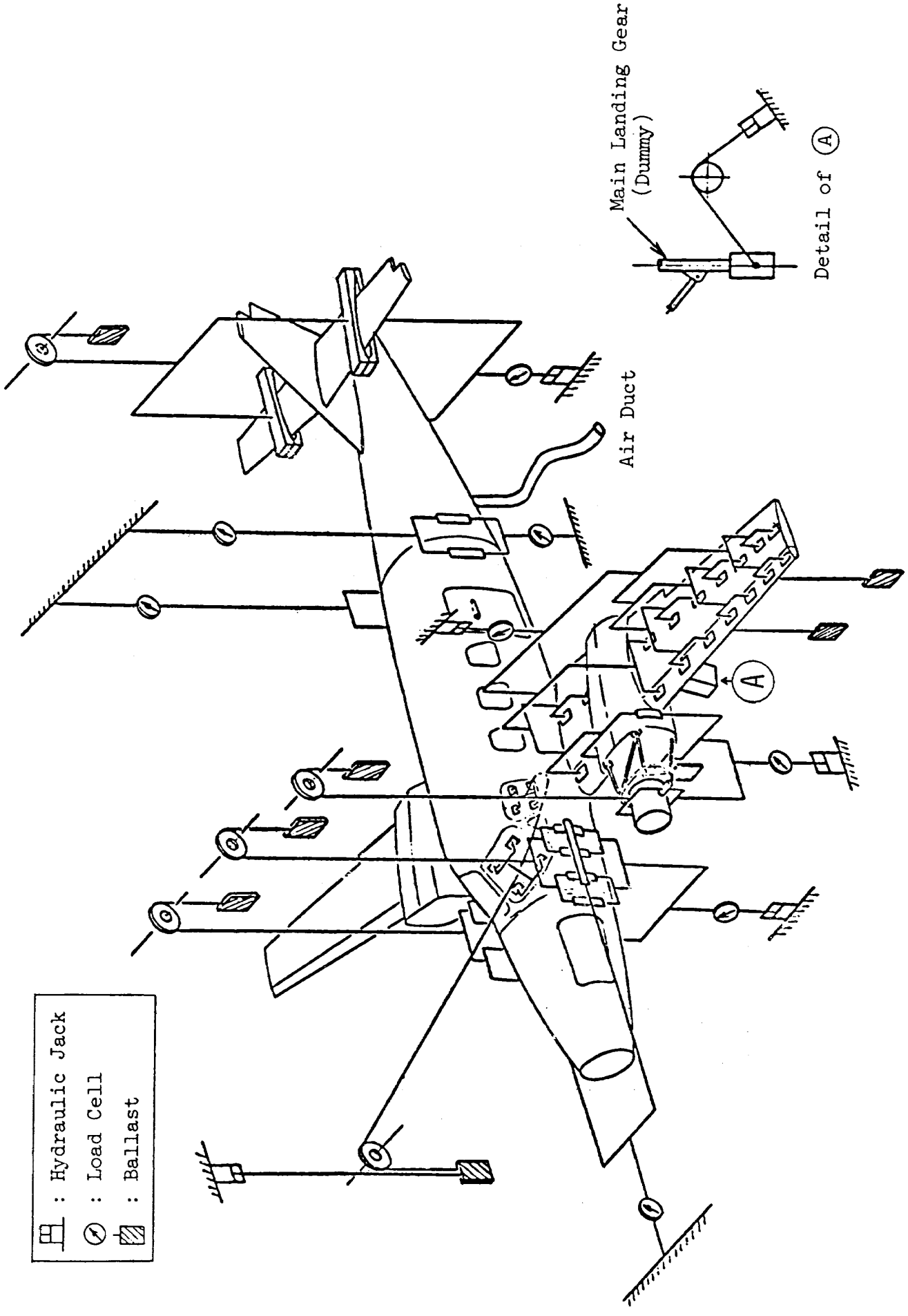

Fig. 21 Full Scale Safe Life Test Setup

Pattern	Freq./240flt
A	160
B	70
C	8
D	1
E	1

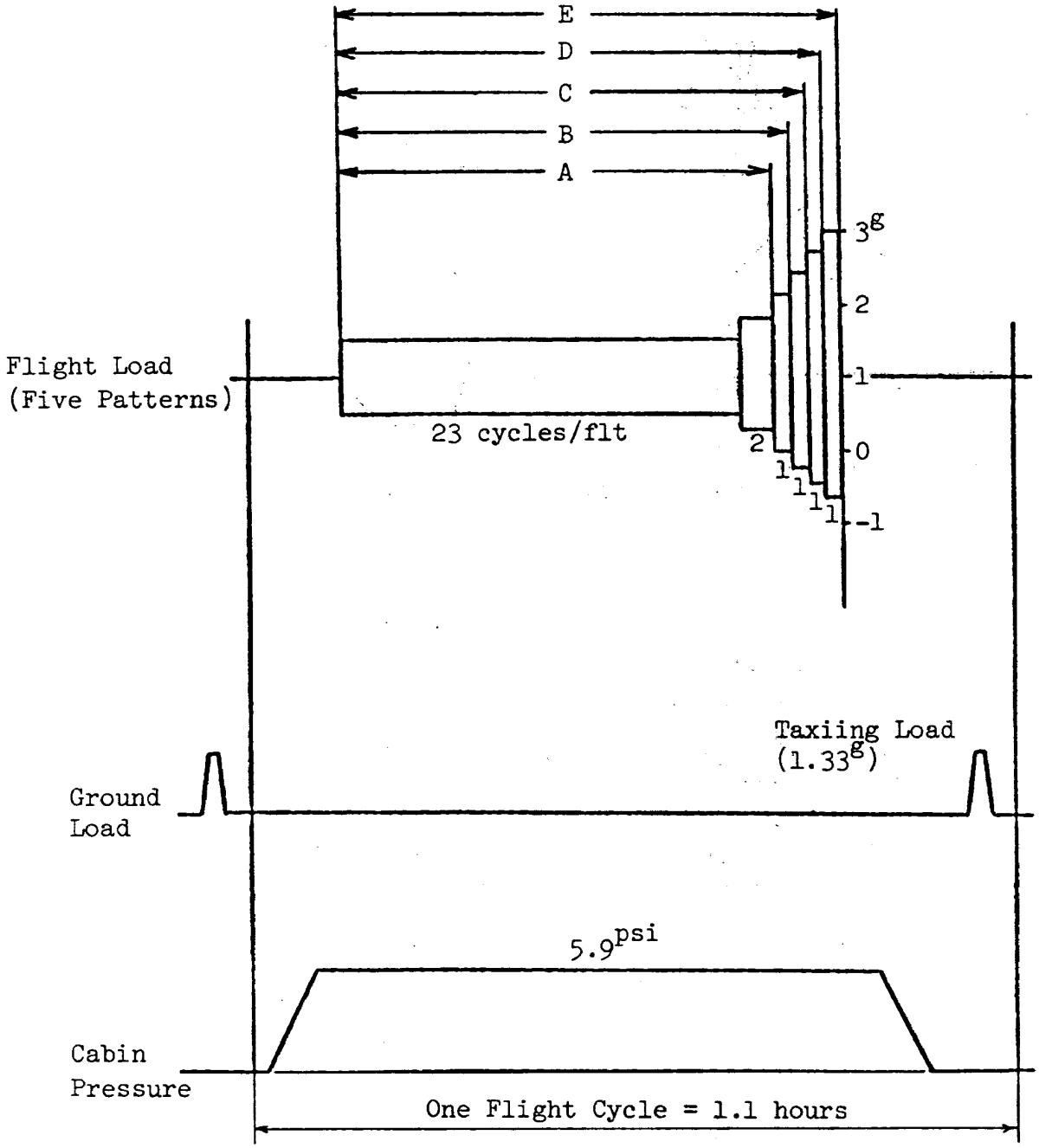

Fig. 22 Loading Pattern of Full Scale Safe Life Test

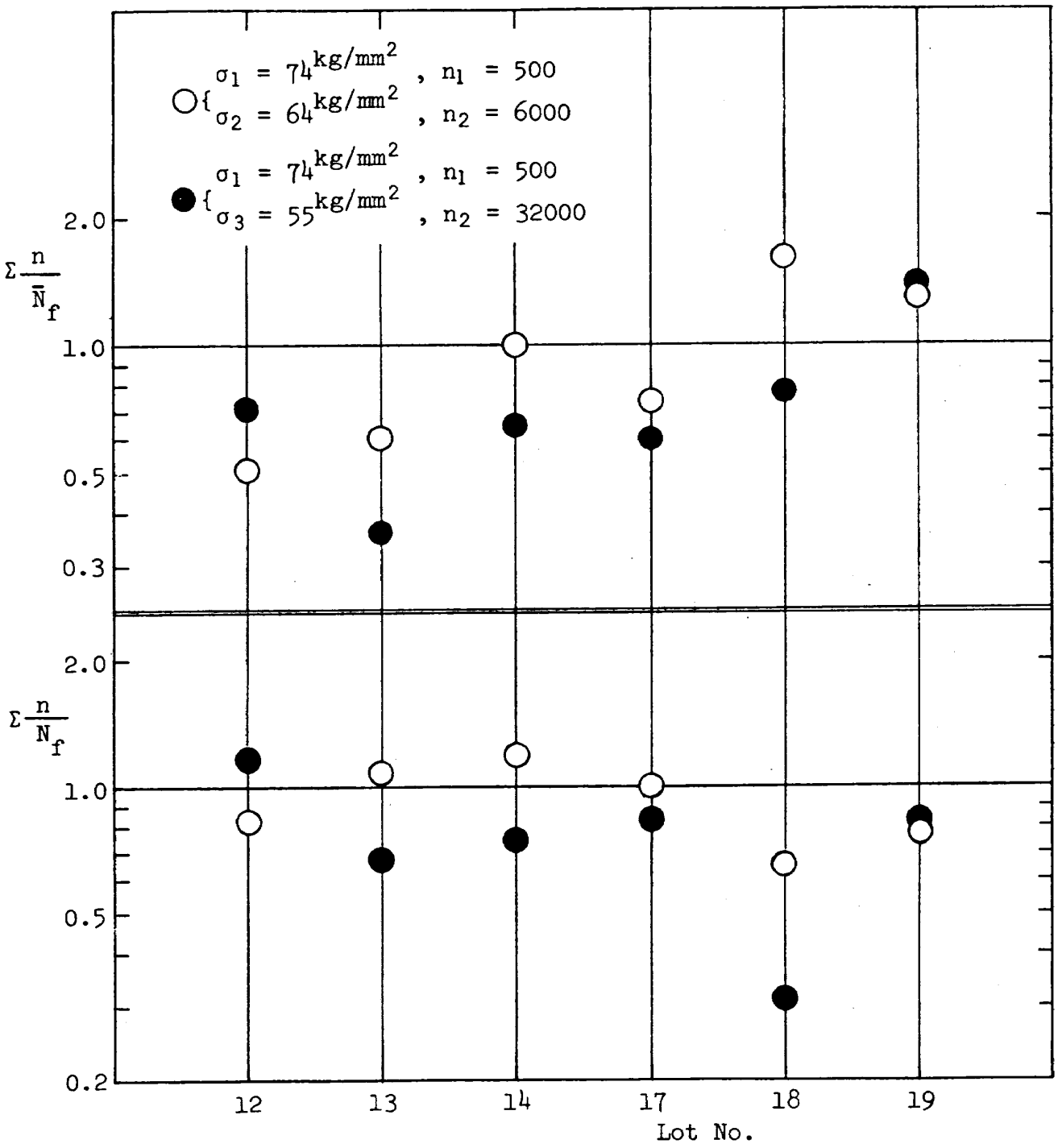

Fig. 23 Results of Spectrum Load Test

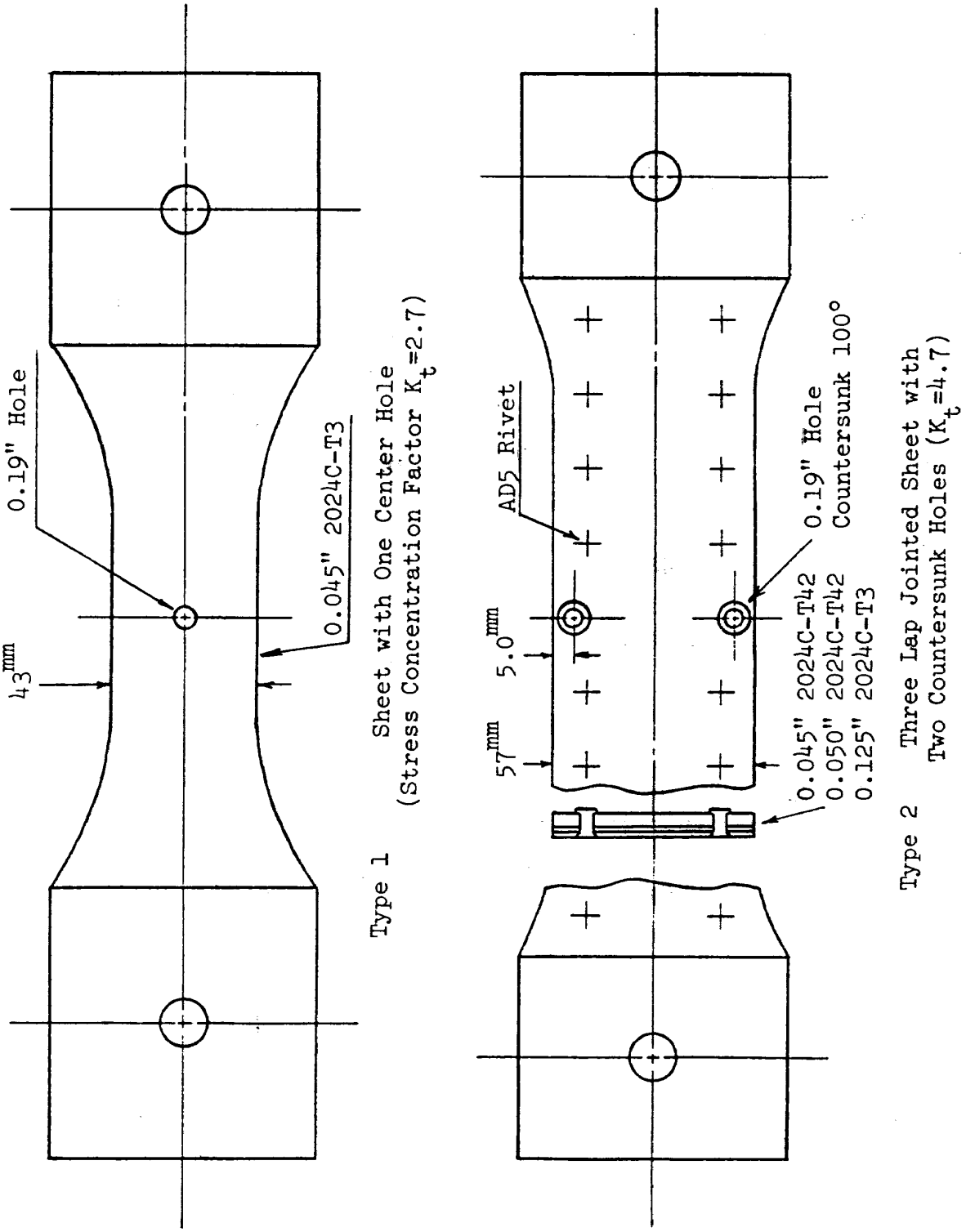

Fig. 24 Test Specimens

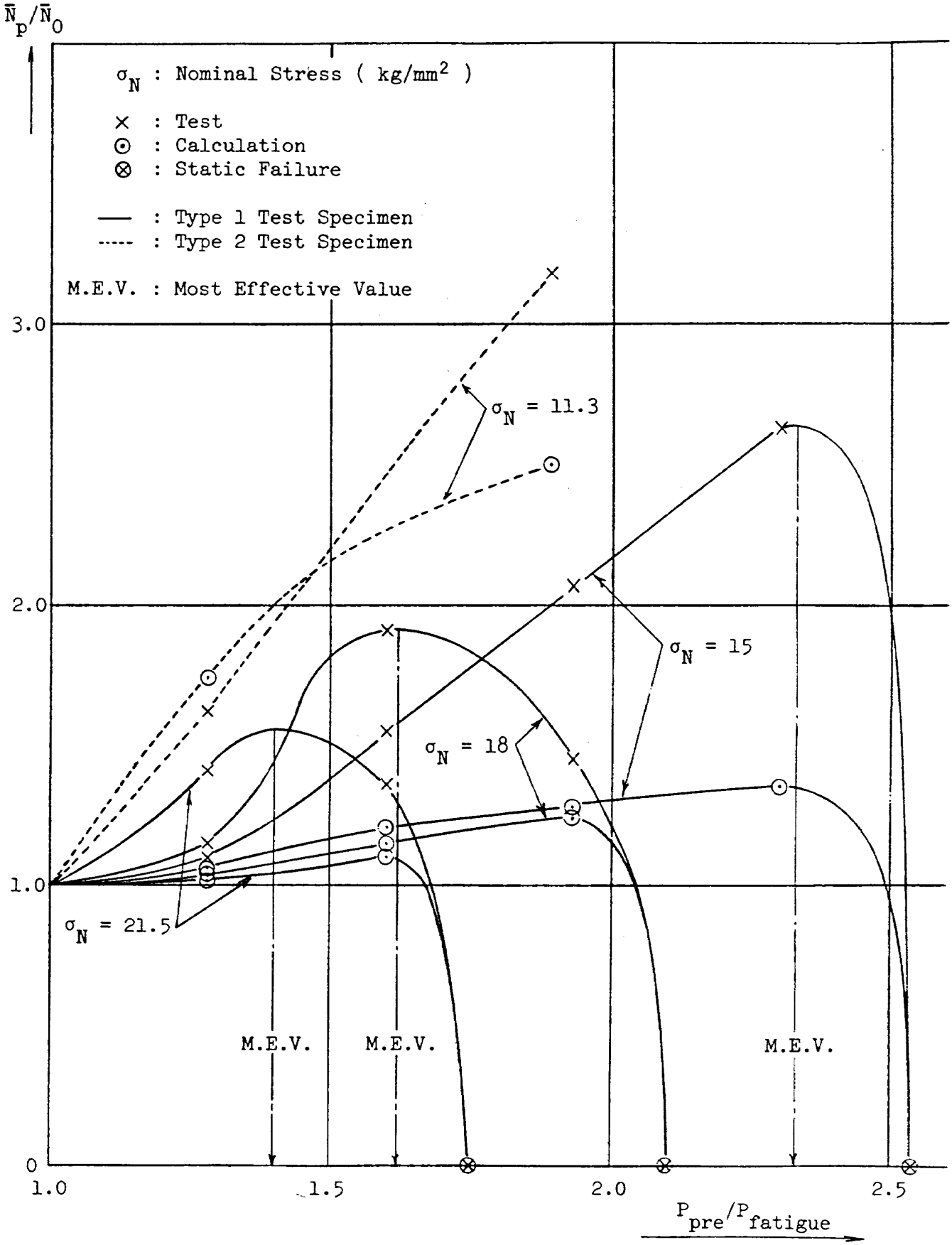

Fig. 25 Relation between Fatigue Life Ratio ($\bar{N}_p/\bar{N}_o$) and Pre-load Ratio ($P_{pre}/P_{fatigue}$)

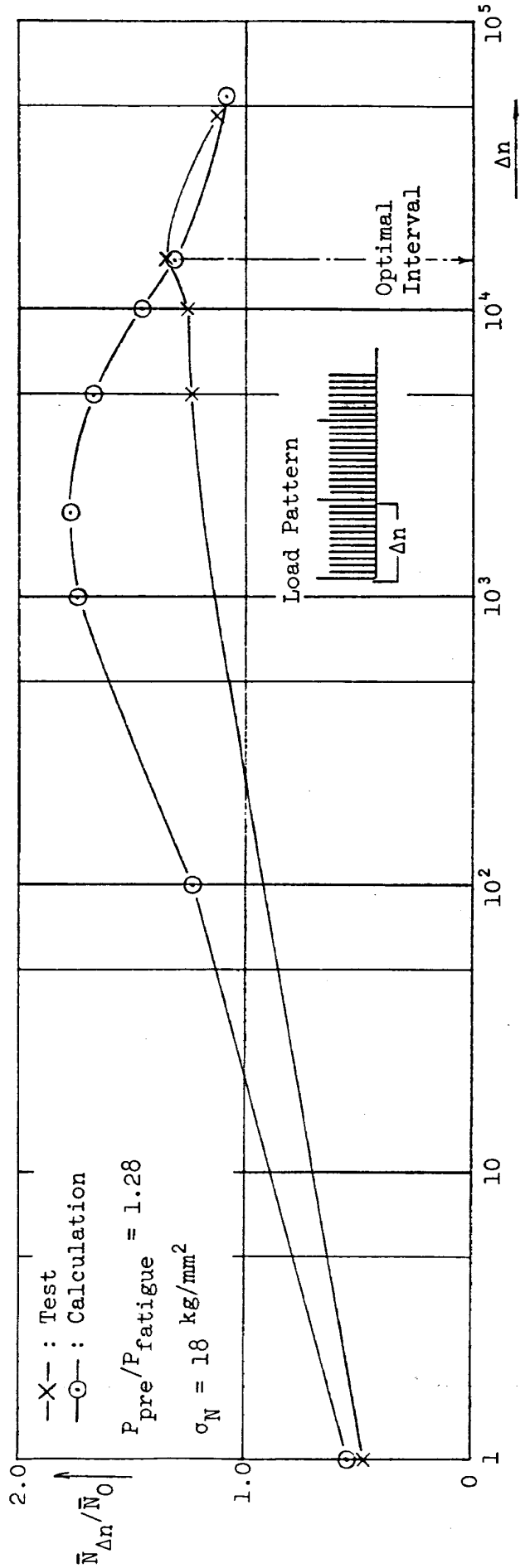

Fig. 26 Relation between $\bar{N}_{\Delta n}/\bar{N}_0$ and Δn (Type 1 Test Specimen)

TECHNICAL MEMORANDUM OF NATIONAL
AEROSPACE LABORATORY
TM-333T

航空宇宙技術研究所資料333T号(欧文)

昭和52年7月発行

発行所　航空宇宙技術研究所
東京都調布市深大寺町1,880
電話 武蔵野三鷹(0422)47-5911(大代表)
印刷所　株式会社　共進
東京都杉並区久我山4-1-7(羽田ビル)

Published by
NATIONAL AEROSPACE LABORATORY
1,880 Jindaiji, Chōfu, Tokyo
JAPAN

Printed in Japan